



Early View

Original research article

***Ex vivo* delivery of regulatory T cells for control of alloimmune priming in the donor lung**

Ei Miyamoto, Akihiro Takahagi, Akihiro Ohsumi, Tereza Martinu, David Hwang, Kristen M. Boonstra, Betty Joe, Juan Mauricio Umana, Ke F. Bei, Daniel Vosoughi, Mingyao Liu, Marcelo Cypel, Shaf Keshavjee, Stephen C. Juvet

Please cite this article as: Miyamoto E, Takahagi A, Ohsumi A, *et al.* *Ex vivo* delivery of regulatory T cells for control of alloimmune priming in the donor lung. *Eur Respir J* 2021; in press (<https://doi.org/10.1183/13993003.00798-2021>).

This manuscript has recently been accepted for publication in the *European Respiratory Journal*. It is published here in its accepted form prior to copyediting and typesetting by our production team. After these production processes are complete and the authors have approved the resulting proofs, the article will move to the latest issue of the ERJ online.

Ex vivo delivery of regulatory T cells for control of alloimmune priming in the donor lung

Authors: Ei Miyamoto, Akihiro Takahagi, Akihiro Ohsumi, Tereza Martinu, David Hwang, Kristen M. Boonstra, Betty Joe, Juan Mauricio Umana, Ke F. Bei, Daniel Vosoughi, Mingyao Liu, Marcelo Cypel, Shaf Keshavjee, Stephen C. Juvet*

Affiliations:

Latner Thoracic Surgery Research Laboratories, University Health Network, University of Toronto, Toronto, Ontario, Canada.

***Corresponding author**

Address: 585 University Avenue, Room 11 PMB 126, Toronto ON Canada M5G 2N2

Tell#: 416-340-4800 (x8178)

Fax#: 416-946-4532

Stephen.Juvet@uhn.ca

Take home message: We developed a recipient-derived lung allograft-directed regulatory T cell therapy administered prior to transplantation. Our results show the feasibility of this approach in rat and human lungs and provide evidence of immune regulation post-transplant.

Abstract:

Survival after lung transplantation (LTx) is hampered by uncontrolled inflammation and alloimmunity. Regulatory T cells (Tregs) are being studied as a cellular therapy in solid organ transplantation. Whether these systemically administered Tregs can function at the appropriate location and time is an important concern. We hypothesized that *in vitro* expanded, recipient-derived Tregs can be delivered to donor lungs prior to LTx via *ex vivo* lung perfusion (EVLP), maintaining their immunomodulatory ability.

In a rat model, Wistar Kyoto (WKy) CD4⁺CD25^{high} Tregs were expanded *in vitro* prior to EVLP. Expanded Tregs were administered to Fisher 344 (F344) donor lungs during EVLP; left lungs were transplanted into WKy recipients. Treg localization and function post-transplant were assessed. In a proof-of-concept experiment, cryopreserved expanded human CD4⁺CD25⁺CD127^{low} Tregs were thawed and injected into discarded human lungs during EVLP. Rat Tregs entered the lung parenchyma and retained suppressive function. Expanded Tregs had no adverse effect on donor lung physiology during EVLP; lung water as measured by wet-to-dry weight ratio was reduced by Treg therapy. The administered cells remained in the graft at 3 days post-transplant where they reduced activation of intragraft effector CD4⁺ T cells; these effects were diminished by day 7. Human Tregs entered the lung parenchyma during EVLP where they expressed key immunoregulatory molecules (CTLA4⁺, 4-1BB⁺, CD39⁺, and CD15s⁺). Pre-transplant Treg administration can inhibit alloimmunity within the lung allograft at early time points post-transplant. Our organ-directed approach has potential for clinical translation.

Introduction

Lung transplantation (LTx) is life-saving in end-stage pulmonary diseases [1]. Unfortunately, despite immunosuppression, median survival after LTx is only 6 years due to chronic lung allograft dysfunction (CLAD), a syndrome of chronic rejection caused by progressive parenchymal and/or small airway fibrosis. CLAD is driven primarily by recipient alloimmunity, which is augmented by ischemia-reperfusion injury, infection, air pollution and microaspiration. While antifibrotic therapies may slow CLAD progression, CLAD prevention by inhibiting alloimmunity is likely to have a greater impact on LTx outcome. Hence, control of the inflammatory tone within the allograft is of paramount importance to preserving long term lung function in LTx recipients.

CD4⁺CD25^{hi}Foxp3⁺ regulatory T cells (Tregs) can inhibit allograft rejection and are being studied as a systemic cellular therapy in clinical trials of kidney and liver transplantation [2]. Treg therapy for living-donor kidney transplant recipients is safe and feasible, but its efficacy is not established [3]. Although lymphoid organs are a key site of Treg function, a high Treg-to-conventional T cell (Tconv) ratio within allografts is required for allograft acceptance [4, 5]. Moreover, lung allografts can be rejected in the absence of secondary lymphoid organs, and the graft is the initial site of alloreactive T cell priming [6, 7]. Tregs can control alloimmunity within the lung allograft [8], and prior arrival of Tregs may provide even more potent control over Tconv activation than when the cells arrive simultaneously [9, 10]. Thus, post-transplant systemic Treg administration in LTx recipients may not provide timely immune regulation at relevant sites *in vivo*.

We have developed and translated to the bedside, a technique of extended *ex vivo* lung perfusion (EVLVP) for donor lung assessment and treatment [11] and for delivery of gene and cellular therapies in animal and human lungs [12, 13]. Pre-transplant administration of recipient-derived Tregs directly into donor lungs affords the opportunity to seed the allograft with therapeutic immune regulatory cells in advance of the arrival of alloreactive T cells after graft implantation.

Since Tregs can be expanded, cryopreserved and thawed at a later date while retaining function [14], this approach is suitable for LTx from deceased donors.

Here, using a rat model, we tested the hypothesis that *in vitro* expanded recipient Tregs administered to the donor lung allograft during EVLP prior to transplantation creates an immunoregulatory environment in the lung leading to a diminished anti-donor immune response post-implantation. In a proof-of-concept experiment, we further showed that cryopreserved expanded human Tregs can be delivered successfully to human lungs on EVLP. Our findings have important implications for the use of lung-directed cellular therapies in transplantation and beyond.

Materials and Methods

Expanded rat Treg injection during rat EVLP followed by LTx

We opted for a rat model amenable to EVLP followed by single LTx, based on prior experience (figure 1a) [15, 16]. We used the Fisher 344 (F344, RT1^{lv})-to-Wistar Kyoto (WKy, RT1^l) strain combination [17]. WKy CD4⁺CD25^{high} cells were isolated by magnetic and fluorescence-activated cell sorting and expanded with anti-CD3 and anti-CD28 coated beads (Miltenyi Biotec) and 1000 units/mL recombinant human IL-2 (rhIL-2, Chiron) for 7 days. Expanded Tregs were labelled with (5-(and 6)-(((4-chloromethyl)benzoyl)amino)tetramethylrhodamine) (CMTMR; CellTracker Orange) and/or eFluor 450 (eF450) cell tracker dye and resuspended in 1 mL Steen® solution (XVIVO Perfusion, Denver, CO). Normothermic acellular EVLP was performed as previously reported [15]. A total of $4.3\text{--}211.3 \times 10^6$ live Tregs/kg F344 donor body weight were injected into the EVLP circuit upstream of the lungs at 60 min of EVLP. Control grafts received 1 mL Steen® containing no cells. Perfusate was sampled upstream and downstream of the lung. At 180 min after injection, the right lung was used for analysis and the left lung was transplanted into a WKy recipient. Recipients were euthanized at days 3 or 7 post-transplant. The animal study was

performed in accordance with the Canadian Council on Animal Care, and the protocol was approved by the Institutional Animal Care Committee (protocol 2853).

Expanded human Treg injection during human EVLP

The human protocol is shown in figure 1b. Healthy donor CD4⁺CD25⁺CD127^{low} cells were expanded for 21 days using anti-CD3 and anti-CD28-coated beads (Miltenyi Biotec) and 300 units/mL rhIL-2, and were cryopreserved. Human donor lungs (n=3) on normothermic acellular EVLP and deemed unsuitable for transplantation due to edema and/or poor compliance were used. Left or right single lung EVLP was established by clamping the hilum of the worse lung. Cryopreserved Tregs were thawed and labelled with CMTMR and eF450, and a total of 0.4–0.8 × 10⁹ were injected in 20 mL Steen into the EVLP circuit upstream of the lung. Tissue samples taken at similar time points from contemporaneous declined lungs undergoing EVLP (no Treg injection, n = 5) were obtained as controls. Experiments using human lungs and healthy donor blood were performed in accordance with the Helsinki declaration and were approved by the Institutional Research Ethics Board (protocols 06-283 and 17-6229, respectively).

Results

Characteristics of isolated and expanded rat Tregs

We sorted WKy CD4⁺CD25^{high} cells (highest 2% of CD25⁺ CD4⁺ T cells, supplementary figure 1a) and found that they were 73.4 ± 12.8% Foxp3⁺. Whereas human Tregs are CD4⁺CD25^{high}CD127^{low}, CD127 and FoxP3 expression were unrelated in rat CD4⁺ T cells (not shown). Expansion with anti-CD3 and anti-CD28-coated beads and IL-2 resulted in 152.8 ± 17.1-fold expansion (figure 2a, n = 21), with largely retained FoxP3 (63.5 ± 8.3% FoxP3⁺, supplementary figure 1b) and CD25 expression (93.6 ± 1.5% CD25⁺, supplementary figure 1c) at day 7. Tregs upregulated CD8 (81.3 ± 2.4% CD8⁺, supplementary figure 1d) at day 7, as reported [18]. Expanded Tregs dose-dependently suppressed *in vitro* proliferation of polyclonally

stimulated CD4⁺CD25^{low} Tconv (figure 2b). Beyond 7 days of expansion, the proportion of FoxP3-expressing T cells decreased (not shown) and so in all rat experiments, cells were used at day 7 of expansion.

Interaction of Tregs with lung allografts during rat EVLP

Tregs were tracked during EVLP (supplementary figure 1f-g) by dye labeling (figure 3a). The proportion of live Tregs rapidly increased in both pulmonary artery (PA) and vein (PV) perfusate after injection and plateaued within 60 min (figure 3b). Remarkably, ~25% of administered Tregs remained in the EVLP circuit after EVLP regardless of cell dose (figure 3c). Treg infusion did not affect lung compliance (figure 3d), vascular resistance (figure 3e), or mean PA pressure (figure 3f). Gas exchange – measured by the ratio of the arterial partial pressure of oxygen to the fraction of inspired oxygen (PaO₂/FiO₂, figure 3g) – and perfusate glucose and lactate concentrations (supplementary figure 2a-b) were unaffected by Treg infusion.

Administered Tregs enter lung allografts and reduce lung vascular permeability at end of EVLP

Acute lung injury scores did not differ between Treg-treated lungs and controls after EVLP (figure 4a; supplementary figure 2c). The wet-to-dry weight ratio was lower in Treg-treated lungs (figure 4b), suggesting that Tregs may have reduced lung edema; however, zonula occludens-1 (ZO-1) staining, a measure of alveolar tight junction integrity, was similar among Treg-treated lungs and controls (supplementary figure 2d).

After EVLP, CMTMR⁺ Tregs were seen outside CD31⁺ vascular structures in the parenchyma (figure 4c). Tregs dose-dependently entered the lung, without evidence of saturation in the range of doses tested (figure 4d). CMTMR⁺ eF450⁺ Tregs sorted from digested lung tissue at the end of EVLP (supplementary figure 2e) suppressed the proliferation of syngeneic polyclonally-stimulated Tconv with a slightly lower potency than Tregs remaining in the EVLP circuit (figure 4e). Compared to control lungs, Treg-treated lungs had higher levels of the Treg-related transcripts

FoxP3, CTLA4, GITR, and CCR4 at the end of EVLP (figure 4f and supplementary figure 2f). There was no difference in the rate of apoptosis, as measured by TUNEL staining, in Treg-treated lungs up to 200 million Tregs/kg donor body weight, compared to controls (supplementary figure 2g). Further, Tregs themselves were not apoptotic at the end of EVLP ($0.97 \pm 0.52\%$, supplementary figure 2h).

Transferred Tregs remain functional in the recipient post-transplant

Transferred Tregs were detectable in the lung at day 3 post-transplant (figure 5a; supplementary figure 3a-b). Compared to the end of EVLP, the cells had shifted to a predominantly subpleural, rather than a perihilar location (figure 5b). Tregs mediate contact-dependent modulation of major histocompatibility complex (MHC) class II⁺ antigen-presenting cells [19]; the percentage of Tregs adjacent to MHC class II-expressing cells in the graft was increased on day 3 compared to at the end of EVLP (figure 5c). Further, FoxP3 expression by CD4⁺ T cells was higher in Treg-treated allografts than in controls at this time (figure 5d; supplementary figure 3c-d). Untreated lungs exhibited a lesser increase in allograft Treg content at day 3, as has been reported in other transplantation settings [20]. Transferred Tregs were also identified in the draining lymph nodes (dLNs) on day 3, within the extravascular space (figure 5e and supplementary figure 3e).

At day 3 post-transplant, acute lung injury scores did not differ between Treg-treated grafts and controls, with only mild abnormalities in both groups (figure 6a-b; supplementary figure 4a). The number of CD3⁺ Tconv cells adjacent to MHC class II⁺ cells was reduced in Treg-treated lungs compared to controls on day 3 (figure 6c-d). Moreover, within Treg-treated lung allografts, fewer CD3⁺ Tconv cells were adjacent to MHC class II⁺ cells that were closely associated with transferred Tregs in comparison with those that were not (figure 6e).

The percentage of CD3⁺ T cells among live cells at day 3 post-transplant was decreased by Treg treatment (figure 6f and supplementary figure 4c). Upregulation of ICAM1 and CD44 and downregulation of CD62L correlate with rat Tconv activation [21–23]. We observed distinct

populations of ICAM1⁺, CD62L⁻, or CD44⁺ Tconv in the lungs and dLNs at day 3 (supplementary figure 4d-i). Treg administration during EVLP reduced both the ICAM1⁺CD44⁺ subset (figure 6g-h) and the ICAM1⁺CD62L⁻ subset (supplementary figure 4j-k) of CD4⁺ T cells in the graft and LNs. In contrast, the CD44⁺CD62L⁻ subset of CD4⁺ T cells was decreased by Treg in the LNs, but not in the lung graft (supplementary figure 4l-m). ICAM1⁺CD62L⁻ CD8⁺ T cells were also decreased by Treg treatment in the lung graft, but not in the LNs (figure 6i-j). FoxP3 and Granzyme B were still elevated in Treg-treated lung grafts at day 3 post-transplant compared to controls (supplementary figure 4n), but not in the dLNs (supplementary figure 4o).

At day 7 post-transplant, acute lung injury and lung allograft rejection scores (ISHLT A and B grades) were similar between Treg-treated lungs and controls (supplementary figure 5a-b). CD4⁺ T cell numbers were reduced in Treg-treated allografts, although this observation did not reach statistical significance (figure 7a; supplementary figure 5c). Our ability to detect transferred cells at day 7 was impaired, perhaps due to loss of labelling dye. Nevertheless, FoxP3 expression in CD4⁺ T cells remained higher in Treg-treated allografts, compared to controls (figure 7b and supplementary figure 5d). CD90 is upregulated on activated rat T cells [24], and we observed fewer CD90⁺ CD4⁺ T cells in the lung allograft at day 7 (figure 7c; supplementary figure 5d); reductions in CD90⁺CD4⁺ T cells were also seen in the dLNs but these findings were not statistically significant. No difference in Treg-related transcripts was observed between Treg-treated lung grafts and controls at day 7 post-transplant (supplementary figure 5e).

Administration of allogeneic human Tregs during human EVLP

Human Tregs expanded $1,067.7 \pm 363.4$ -fold and were $96.3 \pm 1.2\%$ viable after 21 days in culture (supplementary table 1). Viable cells were $81.4 \pm 4.7\%$ FoxP3⁺ and $81.8 \pm 5.3\%$ CTLA4⁺ (figure 8a). Lung donor characteristics and EVLP parameters are shown in supplementary table 2. Injected Tregs were $87.1 \pm 1.2\%$ viable and $80.2 \pm 6.7\%$ CD4⁺CD127^{low}. EVLP perfusate measurements are shown in supplementary table 1. Transferred Tregs were identifiable in

perfusate and lung tissue samples obtained 1h after injection (figure 8b-c; supplementary figure 6c). Expression of key functional Treg markers CTLA4, CD15s, CD39, 4-1BB, and CXCR4 was higher in lung than in perfusate Tregs 1h after injection (figure 8d). CCR4 expression was also higher in lung than in perfusate Tregs, although this observation was not statistically significant (figure 8d). Further, although lung Tregs exhibited higher CD40L and CD45RA expression, there was no clear difference in the expression of FoxP3 or several other Treg- and chemokine-related molecules (supplementary figure 6d). In lung tissue, Treg-related transcripts IL-10, Granzyme B, and IDO-1 increased 1h after Treg injection compared to controls over a similar period on EVLP (figure 8e). Interestingly, FoxP3 and CTLA4 were not consistently upregulated in Treg-treated lungs compared to controls (supplementary figure 6e).

Discussion

EVLP assessment of graft function prior to LTx has expanded the donor pool, with short- and long-term outcomes equivalent to conventional LTx [25]. EVLP also holds promise as a tool for delivery of advanced cell and gene therapies to reduce lung allograft injury [12, 26]. Furthermore, it provides an opportunity to immunologically manipulate the donor organ in the recipient's favor, prior to the arrival of recipient leukocytes. With this concept in mind, we used EVLP to examine whether pre-transplant administration of expanded recipient Tregs to the graft could modify the alloimmune response at its earliest stages.

We successfully expanded suppressive rat CD4⁺CD25^{high} Tregs with properties comparable to mouse and human Tregs [27, 28]. The cells were not harmful across a wide range of doses; ~25% of the administered cells remained in the EVLP circuit irrespective of dose. Chemokine receptors can promote Treg entry into tissues [29]. We found that CXCR4, but not CCR5, CCR6, CCR7 or CXCR3, were more highly expressed on Tregs entering human lungs than those remaining in the EVLP circuit. CCR4 expression was also higher in lung than in perfusate Tregs, and although this finding was not statistically significant, the rat and human data collectively suggest that CXCR4

and CCR4 may be involved in migration of the cells into the lung. Whereas T cell receptor (TCR)-MHC interaction mediates CD8⁺ T cell uptake by allografts [30], its role in CD4⁺ T cell uptake is less clear [31, 32] and moreover, only ~5-15% of T cells are alloreactive [33–36], suggesting that Treg uptake was not strictly TCR-dependent. The roles of chemokine receptors and the TCR in Treg entry to lung allografts remain uncertain and will require further study.

Tregs entered the parenchyma without causing injury. Movement of water out of pulmonary capillaries into the interstitium and alveolar spaces contributes to lung injury and primary graft dysfunction after LTx [37, 38]. Typically, the alveolar-capillary barrier is disrupted, which can be revealed by ZO-1 staining [12]. Although lung water was reduced in Treg-treated lungs compared with controls, ZO-1 staining was not altered at the end of EVLP despite our prediction that Tregs might have promoted improved alveolar-capillary barrier integrity. The degree of injury in these lungs may have been too mild to detect meaningful differences, since the wet-to-dry weight ratio of control lungs was also near normal [39]. It is conceivable that Tregs may have altered one or more physiologic alveolar fluid clearance pathways [40]. Whether polyclonally-expanded Tregs can repair damaged lungs is an important question that awaits further investigation.

Intra-graft immune regulatory transcripts were increased after Treg infusion in the rat (FoxP3, CTLA4, CCR4 and GITR) and human (IL-10, IDO-1) models, and Tregs sorted from treated rat lungs retained suppressive function, although with lower potency than Tregs remaining in the perfusate. This difference might reflect reduced viability or loss of functional molecules caused by enzymatic digestion, or indicate that Tregs entering the lung were intrinsically less functional. Nevertheless, they continued to exert immune regulation *in vivo* post-transplant. At day 3, they exhibited increased proximity to antigen presenting cells (APCs), the principal site of immune regulation by Tregs *in vivo* [19]. Recipient Tconv, in contrast, displayed reduced proximity to APCs in the presence of Tregs, with Treg-associated APCs showing the lowest proximity to Tconv. Further, Tconv in Treg-treated lungs and dLNs exhibited reduced T cell activation marker

expression compared to controls. These are important findings, since lung allograft CD11c⁺ APCs are the initial site of T cell priming, which has already occurred by day 3 post-transplant [6]. Collectively, these data support the concept of pre-transplant Treg delivery to the organ.

For polyclonal Treg therapies, such as the ones used here, it is estimated that a 1:1 or 1:2 Treg:Tconv ratio is required within the target organ to inhibit rejection [41]. To achieve this ratio with systemic Treg administration might be difficult, but our approach boosted the Treg-to-Tconv ratio in the graft from 1:5 up to 1:2 at 3 days post-transplant (figure 5d), suggesting a means by which to attain this goal.

Transplanted lungs are directly exposed to the external environment via the airways, rendering them susceptible to inflammatory stimuli that enhance risks for rejection and CLAD [42–44]. Intra-graft immune regulatory mechanisms are therefore likely to be even more important in LTx than in other transplanted organs. While our approach resulted in ~40% of CD4⁺ T cells expressing FoxP3 at day 3 post-LTx (figure 5d), only ~10% expressed FoxP3 at day 7 (figure 7d), which may explain why we did not observe an impact on acute rejection at day 7. Indeed, lung allograft residency by Tregs is likely to be required for lung allograft acceptance [45], and we speculate that ongoing engagement of peripheral tolerance mechanisms in the graft will be needed to prevent rejection after LTx.

Our study has several limitations. Only a minority of polyclonal Tregs are reactive to donor antigens, and further, we cannot be certain that the reduced Tconv activation seen in the presence of Tregs was strictly due to control of the alloimmune response, since we did not assess these phenomena in a syngeneic control group. Ultimately, since donor antigen-reactive Tregs are more potent than polyclonal Tregs [46], it would be desirable to combine our approach with chimeric antigen receptors [47, 48]. We did not administer immunosuppressive drugs, and since calcineurin inhibitors can limit Treg function [49], it is likely that standard LTx immunosuppression would reduce effectiveness. We did not evaluate the resistance of the Tregs to conversion to

harmful effector cells; however, we used naturally-occurring (originating in the thymus) Tregs in our study, which are more stable than *in vitro* induced Tregs [45]. Future work will be needed to evaluate Treg stability in this context. We were unable to track administered cells beyond day 3, perhaps due to dilution of labeling dyes and/or cell death or migration; nevertheless, FoxP3⁺ cells were more prevalent among CD4⁺ T cells in Treg-treated grafts compared with controls at 7 days post-transplant. Selective immunosuppressive approaches to enhance Treg responses are emerging [50, 51] and it would be attractive to combine one of them with pre-transplant Treg administration.

In summary, recipient-derived expanded Tregs can be administered to rat and human lungs during EVLP. The cells did not injure the grafts and inhibited Tconv responses *in vitro* and *in vivo*. Our findings therefore support the concept that immune modulation can begin in the allograft prior to transplantation, opening the door to personalized organ-directed immunoregulatory cell therapy.

Financial Disclosure Statement: This work was supported by an Ontario Institute for Regenerative Medicine – Medicine by Design New Ideas Grant (#NI17-107) and the Cystic Fibrosis Canada Marsha Morton New Investigator Award (#559984) (both to S.J.). E.M. was supported by Research fellowships from The Cell Science Research Foundation (Japan, 2016), The Kyoto University Foundation (Japan, 2016), and the International Society for Heart and Lung Transplantation (2018). M.C. and S.K. are co-founders of Perfusix Canada, Traferox Technologies Inc. Toronto, and consultants for Lung Bioengineering and United Therapeutics. All other authors declare no competing interests.

Author contributions: S.J. conceived and designed the project. S.J., E.M., A.T., M.C., T.M., M.L., and S.K. contributed to the interpretation of data and critically revised the manuscript. E.M. and A.O. developed the method of rat Treg injection. E.M. and A.T. performed rat EVLP and transplantation. E.M., K.M.B., M.U. and B.J. isolated and expanded Tregs and performed suppression assays and flow cytometry. D.H and T.M. performed histologic grading of acute lung injury in the lung graft. E.M., K.F.B., D.V., and Z.G. performed immunohistochemistry and immunofluorescence staining and analysis. Z.G. performed gene expression analysis. E.M. and S.J. contributed to the statistical analysis.

Acknowledgments:

We thank Toronto General Hospital EVLP team for supporting the human EVLP Treg injection experiments, and The Cell Science Research Foundation (Japan), The Kyoto University Foundation (Japan), and the International Society for Heart and Lung Transplantation for supporting E.M. via their research fellowship programs.

References:

1. Yusen RD, Edwards LB, Dipchand AI, Goldfarb SB, Kucheryavaya AY, Levvey BJ, Lund LH, Meiser B, Rossano JW, Stehlik J. The Registry of the International Society for Heart and Lung Transplantation: Thirty-third Adult Lung and Heart–Lung Transplant Report—2016; Focus Theme: Primary Diagnostic Indications for Transplant. *J Hear Lung Transplant* 2016; 35: 1170–1184.
2. Vaikunthanathan T, Safinia N, Boardman D, Lechler RI, Lombardi G. Regulatory T cells: tolerance induction in solid organ transplantation. *Clin Exp Immunol* 2017; 189: 197–210.
3. Sawitzki B, Harden PN, Reinke P, Moreau A, Hutchinson JA, Game DS, Tang Q, Guinan EC, Battaglia M, Burlingham WJ, Roberts ISD, Streitz M, Josien R, Böger CA, Scottà C, Markmann JF, Hester JL, Juerchott K, Braudeau C, James B, Contreras-Ruiz L, van der Net JB, Bergler T, Caldara R, Petchey W, Edinger M, Dupas N, Kapinsky M, Mutzbauer I, Otto NM, et al. Regulatory cell therapy in kidney transplantation (The ONE Study): a harmonised design and analysis of seven non-randomised, single-arm, phase 1/2A trials. *Lancet* 2020; 395: 1627–1639.
4. Young JS, Yin D, Vannier AGL, Alegre ML, Chong AS. Equal expansion of endogenous transplant-specific regulatory T cell and recruitment into the allograft during rejection and tolerance. *Front Immunol* 2018; 9: 1385.
5. Graca L, Cobbold SP, Waldmann H. Identification of regulatory T cells in tolerated allografts. *J Exp Med* 2002; 195: 1641–1646.
6. Gelman AE, Li W, Richardson SB, Zinselmeyer BH, Lai J, Okazaki M, Kornfeld CG, Kreisel FH, Sugimoto S, Tietjens JR, Dempster J, Patterson GA, Krupnick AS, Miller MJ, Kreisel D. Acute Lung Allograft Rejection Is Independent of Secondary Lymphoid Organs. *J Immunol* 2009; 182: 3969–3973.

7. Wagnetz D, Sato M, Hirayama S, Matsuda Y, Juvet SC, Yeung JC, Guan Z, Zhang L, Liu M, Waddell TK, Keshavjee S. Rejection of tracheal allograft by intrapulmonary lymphoid neogenesis in the absence of secondary lymphoid organs. *Transplantation* 2012; 93: 1212–1220.
8. Li W, Gauthier JM, Tong AY, Terada Y, Higashikubo R, Frye CC, Harrison MS, Hashimoto K, Bery AI, Ritter JH, Nava RG, Puri V, Wong BW, Lavine KJ, Bharat A, Krupnick AS, Gelman AE, Kreisel D. Lymphatic drainage from bronchus-associated lymphoid tissue in tolerant lung allografts promotes peripheral tolerance. *J Clin Invest* 2020; 130: 6718–6727.
9. Nguyen VH, Zeiser R, DaSilva DL, Chang DS, Beilhack A, Contag CH, Negrin RS. In vivo dynamics of regulatory T cell trafficking and survival predict effective strategies to control graft-versus-host disease following allogeneic transplantation. *Blood* 2007; 109: 2649–2656.
10. Zhang P, Tey S-KK, Koyama M, Kuns RD, Olver SD, Lineburg KE, Lor M, Teal BE, Raffelt NC, Raju J, Leveque L, Markey K a, Varelias A, Clouston AD, Lane SW, MacDonald KP a, Hill GR. Induced regulatory T cells promote tolerance when stabilized by rapamycin and IL-2 in vivo. *J Immunol* 2013; 191: 5291–5303.
11. Cypel M, Yeung JC, Mingyao L, Anraku M, Chen F, Karolak W, Sato M, Laratta J, Azad S, Madonik M, Chow CW, Chaparro C, Hutcheon M, Singer LG, Slutsky AS, Yasufuku K, Perrot M De, Pierre AF, Waddell TK, Keshavjee S. Normothermic ex vivo lung perfusion in clinical lung transplantation. *N Engl J Med* 2011; 364: 1431–1440.
12. Cypel M, Liu M, Rubacha M, Yeung JC, Hirayama S, Anraku M, Sato M, Medin J, Davidson BL, De Perrot M, Waddell TK, Slutsky AS, Keshavjee S. Functional repair of human donor lungs by IL-10 gene therapy. *Sci Transl Med* 2009; 1: 4ra9.

13. Mordant P, Nakajima D, Kalaf R, Iskender I, Maahs L, Behrens P, Coutinho R, Iyer RK, Davies JE, Cypel M, Liu M, Waddell TK, Keshavjee S. Mesenchymal stem cell treatment is associated with decreased perfusate concentration of interleukin-8 during ex vivo perfusion of donor lungs after 18-hour preservation. *J Hear Lung Transplant* 2016; 35: 1245–1254.
14. Nadig SN, Wickiewicz J, Wu DC, Warnecke G, Zhang W, Luo S, Schiopu A, Taggart DP, Wood KJ. In vivo prevention of transplant arteriosclerosis by ex vivo-expanded human regulatory T cells. *Nat Med* 2010; 16: 809–813.
15. Ohsumi A, Kanou T, Ali A, Guan Z, Hwang DM, Waddell TK, Juvet S, Liu M, Keshavjee S, Cypel M. A Method for Translational Rat Ex vivo Lung Perfusion Experimentation. *Am J Physiol Lung Cell Mol Physiol* 2020; 319: L61–L70.
16. Noda K, Tane S, Haam SJ, Hayanga AJ, D’Cunha J, Luketich JD, Shigemura N. Optimal ex vivo lung perfusion techniques with oxygenated perfusate. *J Hear Lung Transplant* 2017; 36: 466–474.
17. Von Süßkind-Schwendi M, Ruemmele P, Schmid C, Hirt SW, Lehle K. Lung transplantation in the fischer 344-wistar kyoto strain combination is a relevant experimental model to study the development of bronchiolitis obliterans in the rat. *Exp Lung Res* 2012; 38: 111–123.
18. Verma ND, Robinson CM, Carter N, Wilcox P, Tran GT, Wang C, Sharland A, Nomura M, Plain KM, Bishop GA, Hodgkinson SJ, Hall BM. Alloactivation of naïve CD4⁺ CD8⁻ CD25⁺T regulatory cells: Expression of CD8 α identifies potent suppressor cells that can promote transplant tolerance induction. *Front Immunol* 2019; 10: 2397.

19. Tang Q, Adams JY, Tooley AJ, Bi M, Fife BT, Serra P, Santamaria P, Locksley RM, Krummel MF, Bluestone JA. Visualizing regulatory T cell control of autoimmune responses in nonobese diabetic mice. *Nat Immunol* 2006; 7: 83–92.
20. Fan Z, Spencer JA, Lu Y, Pitsillides CM, Singh G, Kim P, Yun SH, Toxavidis V, Strom TB, Lin CP, Koulmanda M. In vivo tracking of “color-coded” effector, natural and induced regulatory T cells in the allograft response. *Nat Med* 2010; 16: 718–722.
21. Mesri M, Liversidge J, Forrester J V. ICAM-1/LFA-1 interactions in T-lymphocyte activation and adhesion to cells of the blood-retina barrier in the rat. *Immunology* 1994; 83: 52–57.
22. Ponta H, Sherman L, Herrlich PA. CD44: From adhesion molecules to signalling regulators. *Nat Rev Mol Cell Biol* 2003; 4: 33–45.
23. Hengel RL, Thaker V, Pavlick M V., Metcalf JA, Dennis G, Yang J, Lempicki RA, Sereti I, Lane HC. Cutting Edge: L-Selectin (CD62L) Expression Distinguishes Small Resting Memory CD4 + T Cells That Preferentially Respond to Recall Antigen. *J Immunol* 2003; 170: 28–32.
24. Paterson DJ, Jefferies WA, Green JR, Brandon MR, Corthesy P, Puklavec M, Williams AF. Antigens of activated rat T lymphocytes including a molecule of 50,000 Mr detected only on CD4 positive T blasts. *Mol Immunol* 1987; 24: 1281–1290.
25. Yeung JC, Krueger T, Yasufuku K, de Perrot M, Pierre AF, Waddell TK, Singer LG, Keshavjee S, Cypel M. Outcomes after transplantation of lungs preserved for more than 12 h: a retrospective study. *Lancet Respir Med* 2017; 5: 119–124.
26. Nakajima D, Watanabe Y, Ohsumi A, Pipkin M, Chen M, Mordant P, Kanou T, Saito T, Lam R, Coutinho R, Caldarone L, Juvet S, Martinu T, Iyer RK, Davies JE, Hwang DM, Waddell TK, Cypel M, Liu M, Keshavjee S. Mesenchymal stromal cell therapy during ex

- vivo lung perfusion ameliorates ischemia-reperfusion injury in lung transplantation. *J Hear Lung Transplant* 2019; 38: 1214–1223.
27. Ward ST, Li KK, Curbishley SM. A method for conducting suppression assays using small numbers of tissue-isolated regulatory T cells. *MethodsX* 2014; 1: 168–174.
 28. Mcmurphy AN, Levings MK. Suppression assays with human T regulatory cells: A technical guide. *Eur J Immunol* 2012; 42: 27–34.
 29. Liston A, Gray DHD. Homeostatic control of regulatory T cell diversity. *Nat Rev Immunol* 2014; 14: 154–165.
 30. Walch JM, Zeng Q, Li Q, Oberbarnscheidt MH, Hoffman RA, Williams AL, Rothstein DM, Shlomchik WD, Kim J V., Camirand G, Lakkis FG. Cognate antigen directs CD8+ T cell migration to vascularized transplants. *J Clin Invest* 2013; 123: 2663–2671.
 31. Krupnick AS, Gelman AE, Barchet W, Richardson S, Kreisel FH, Turka LA, Colonna M, Patterson GA, Kreisel D. Cutting Edge: Murine Vascular Endothelium Activates and Induces the Generation of Allogeneic CD4 + 25 + Foxp3 + Regulatory T Cells. *J Immunol* 2005; 175: 6265–6270.
 32. Kreisel D, Krasinskas AM, Krupnick AS, Gelman AE, Balsara KR, Popma SH, Riha M, Rosengard AM, Turka LA, Rosengard BR. Vascular Endothelium Does Not Activate CD4 + Direct Allorecognition in Graft Rejection. *J Immunol* 2004; 173: 3027–3034.
 33. Noorchashm H, Lieu YK, Rostami SY, Song HK, Greeley SAS, Bazel S, Barker CF, Naji A. A direct method for the calculation of alloreactive CD4+ T cell precursor frequency. *Transplantation* 1999; 67: 1281–1284.
 34. Lalfer M, Chappert P, Carpentier M, Urbain D, Davoust JM, Gross DA. Foxp3+ regulatory and conventional CD4+ T cells display similarly high frequencies of alloantigen-reactive cells. *Front Immunol* 2019; 10: 1–8.

35. Suchin EJ, Langmuir PB, Palmer E, Sayegh MH, Wells AD, Turka LA. Quantifying the Frequency of Alloreactive T Cells In Vivo: New Answers to an Old Question. *J Immunol* 2001; 166: 973–981.
36. Juvet SC, Sanderson S, Hester J, Wood KJ, Bushell A. Quantification of CD4+T Cell Alloreactivity and Its Control by Regulatory T Cells Using Time-Lapse Microscopy and Immune Synapse Detection. *Am J Transplant* 2016; 16: 1394–1407.
37. Pottecher J, Roche AC, Dégot T, Helms O, Hentz JG, Schmitt JP, Falcoz PE, Santelmo N, Levy F, Collange O, Uring-Lambert B, Bahram S, Schaeffer M, Meyer N, Geny B, Lassalle P, Diemunsch P, Massard G, Kessler R, Steib A, Hirschi S, Canuet M, Schuller A, Rosner V, Wirtz G, Weitzenblum E, Dan Vasilescu M, Olland A, Dupeyron JP, Rigolot JC, et al. Increased extravascular lung water and plasma biomarkers of acute lung injury precede oxygenation impairment in primary graft dysfunction after lung transplantation. *Transplantation* 2017; 101: 112–121.
38. Trebbia G, Sage E, Le Guen M, Roux A, Soummer A, Puyo P, Parquin F, Stern M, Pham T, Sakka SG, Cerf C. Assessment of lung edema during ex-vivo lung perfusion by single transpulmonary thermodilution: A preliminary study in humans. *J Hear Lung Transplant* 2019; 38: 83–91.
39. Kondo T, Chen F, Ohsumi A, Hijiya K, Motoyama H, Sowa T, Ohata K, Takahashi M, Yamada T, Sato M, Aoyama A, Date H. β 2-Adrenoreceptor Agonist Inhalation During Ex Vivo Lung Perfusion Attenuates Lung Injury. *Ann Thorac Surg* 2015; 100: 480–486.
40. Huppert LA, Matthay MA. Alveolar Fluid Clearance in Pathologically Relevant Conditions: In Vitro and In Vivo Models of Acute Respiratory Distress Syndrome. *Front Immunol* 2017; 8: 371.

41. Tang Q, Lee K. Regulatory T-cell therapy for transplantation: How many cells do we need? *Curr Opin Organ Transplant* 2012; 17: 349–354.
42. Verleden GM, Glanville AR, Lease ED, Fisher AJ, Calabrese F, Corris PA, Ensor CR, Gottlieb J, Hachem RR, Lama V, Martinu T, Neil DAH, Singer LG, Snell G, Vos R. Chronic lung allograft dysfunction: Definition, diagnostic criteria, and approaches to treatment—A consensus report from the Pulmonary Council of the ISHLT. *J Hear Lung Transplant* 2019; 38: 493–503.
43. Belperio JA, Weigt SS, Fishbein MC, Lynch JP. Chronic Lung Allograft Rejection: Mechanisms and Therapy. *Proc Am Thorac Soc* 2009; 6: 108–121.
44. Husain AN, Siddiqui MT, Holmes EW, Chandrasekhar AJ, Cabe MMC, Radvany R, Garrity ER, McCabe M, Radvany R, Garrity ER, Cabe MMC, Radvany R, Garrity ER. Analysis of Risk Factors for the Development of Bronchiolitis Obliterans Syndrome. *Am J Respir Crit Care Med* 1995; 159: 829–833.
45. Li W, Gauthier JM, Higashikubo R, Hsiao HM, Tanaka S, Vuong L, Ritter JH, Tong AY, Wong BW, Hachem RR, Puri V, Bharat A, Krupnick AS, Hsieh CS, Baldwin WM, Kelly FL, Palmer SM, Gelman AE, Kreisel D. Bronchus-associated lymphoid tissue–resident Foxp3 + T lymphocytes prevent antibody-mediated lung rejection. *J Clin Invest* 2019; 129: 556–568.
46. Sagoo P, Ali N, Garg G, Nestle FO, Lechler RI, Lombardi G. Human regulatory T cells with alloantigen specificity are more potent inhibitors of alloimmune skin graft damage than polyclonal regulatory T cells. *Sci Transl Med* 2011; 3: 83ra42.
47. MacDonald KG, Hoeppli RE, Huang Q, Gillies J, Luciani DS, Orban PC, Broady R, Levings MK. Alloantigen-specific regulatory T cells generated with a chimeric antigen receptor. *J Clin Invest* 2016; 126: 1413–1424.

48. Noyan F, Zimmermann K, Hardtke-Wolenski M, Knoefel A, Schulde E, Geffers R, Hust M, Huehn J, Galla M, Morgan M, Jokuszies A, Manns MP, Jaeckel E. Prevention of Allograft Rejection by Use of Regulatory T Cells With an MHC-Specific Chimeric Antigen Receptor. *Am J Transplant* 2017; 17: 917–930.
49. Akimova T, Kamath BM, Goebel JW, Meyers KEC, Rand EB, Hawkins A, Levine MH, Bucuvalas JC, Hancock WW. Differing effects of rapamycin or calcineurin inhibitor on T-Regulatory cells in pediatric liver and kidney transplant recipients. *Am J Transplant* 2012; 12: 3449–3461.
50. Whitehouse G, Gray E, Mastoridis S, Merritt E, Kodela E, Yang JHMM, Danger R, Mairal M, Christakoudi S, Lozano JJ, Macdougall IC, Tree TIMM, Sanchez-Fueyo A, Martinez-Llordella M. IL-2 therapy restores regulatory T-cell dysfunction induced by calcineurin inhibitors. *Proc Natl Acad Sci* 2017; 114: 7083–7088.
51. Sockolosky JT, Trotta E, Parisi G, Picton L, Su LL, Le AC, Chhabra A, Silveria SL, George BM, King IC, Tiffany MR, Jude K, Sibener L V., Baker D, Shizuru JA, Ribas A, Bluestone JA, Garcia KC. Selective targeting of engineered T cells using orthogonal IL-2 cytokine-receptor complexes. *Science* 2018; 359: 1037–1042.

Figure legends:

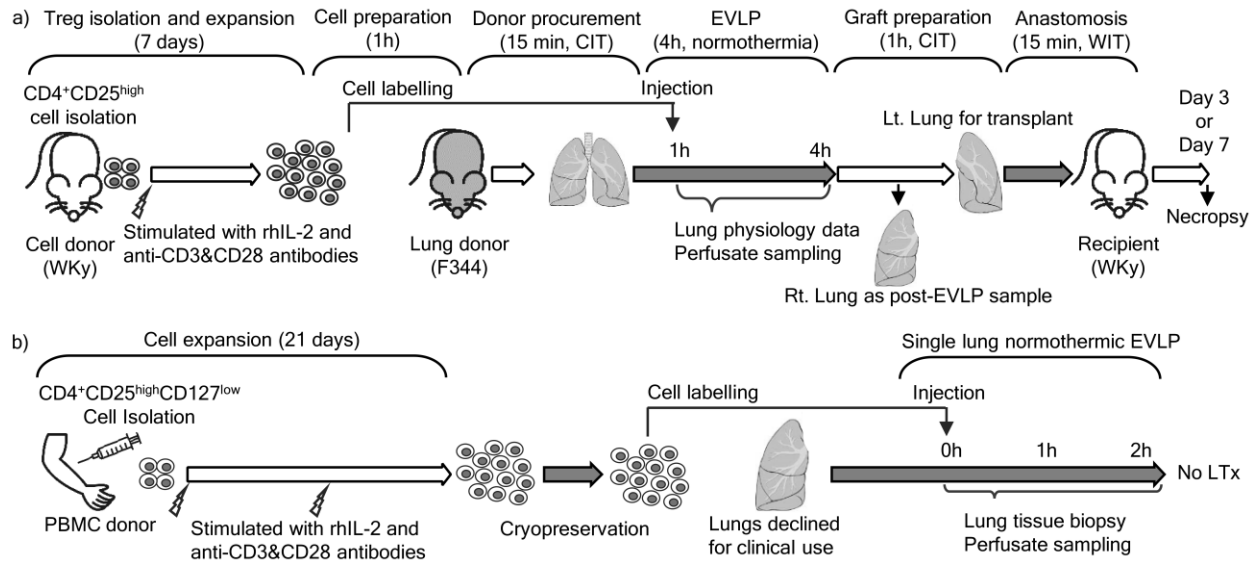


Figure 1. Study protocols.

(a) Schematic of rat Treg experiment. CD4⁺CD25^{high} cells (supplementary figure 1a) were isolated from WKy rat lymph nodes and expanded with rhIL-2 and anti-CD3 and CD28 antibodies for 7 days. Prior to starting EVLP with a F344 rat heart and lung block, the expanded cells were dye labelled for injection. Labelled Tregs or perfusate vehicle were injected to the circuit at the PA port 1 hour after the start of EVLP. After 4 hours, the left lung graft was transplanted to a WKy recipient while the right lung was subjected to further analyses. (b) Schematic of human Treg experiment. CD4⁺CD25^{high}CD127^{low} cells from a healthy blood donor were isolated and expanded *in vitro*. After 21 days, the expanded Tregs were cryopreserved in liquid nitrogen. Upon notification that a lung was declined for transplantation on EVLP, Tregs were rapidly thawed, labeled with CMTMR and eF450, washed and injected into the EVLP circuit (supplementary figure 6b). EVLP continued for up to 2 hours after Treg injection, at which point tissue and perfusate were analyzed. Treg, regulatory T cell; EVLP, ex vivo lung perfusion; CIT, cold ischemic time; WIT, warm ischemic time; WKy, Wistar Kyoto; F344, Fisher 344; rhIL-2, recombinant human IL-2; Lt, left; Rt, right; PBMC, peripheral blood mononuclear cells.

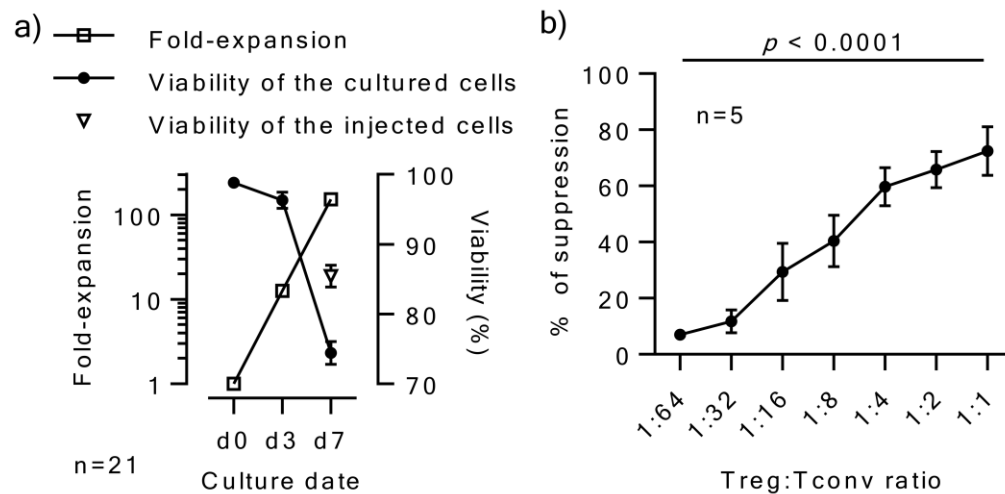


Figure 2. *In vitro* expansion of suppressive WKy Tregs.

(a) Treg expansion (n = 21). Fold-increase and viability of expanded Tregs on day 3 and day 7 of culture shown. Expanded cells were washed, increasing the viable proportion of injected cells to > 80%. (b) WKy Tregs mediate dose-dependent suppression of autologous Tconv (n = 5, $p < 0.0001$, ANOVA). Gating strategy to identify CFSE-labelled Tconv is shown in supplementary figure 1c. Treg, regulatory T cell; Tconv, conventional T cells; CFSE, carboxyfluorescein succinimidyl ester.

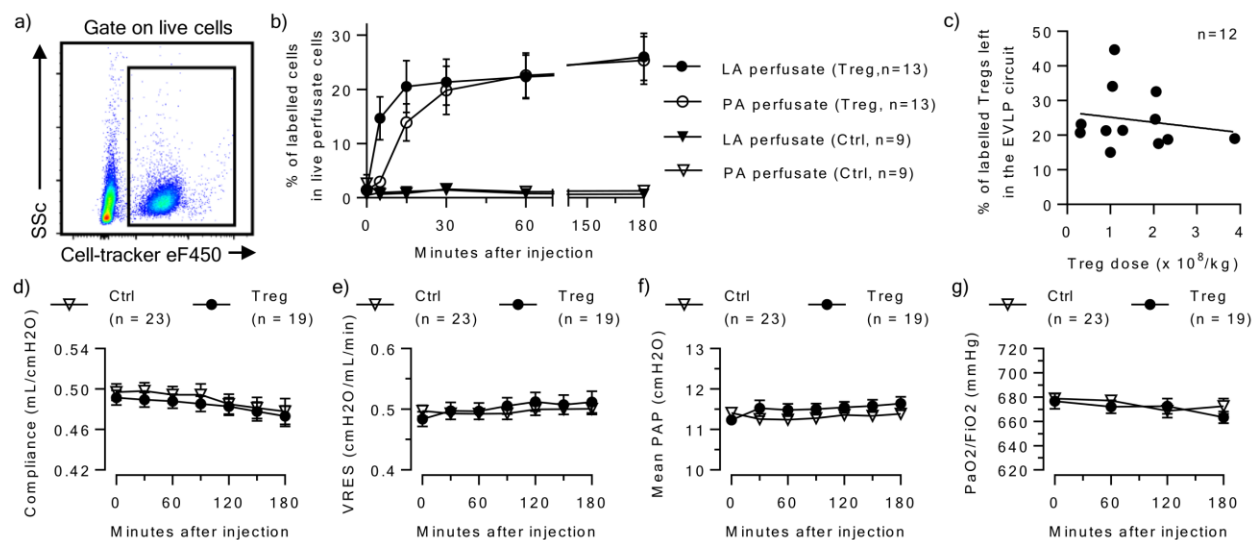


Figure 3. Administration of expanded WKy Tregs to allogeneic F344 lungs during EVLP.

(a) Identification of labelled Tregs in EVLP perfusate by flow cytometry. (b) Proportion of Tregs in live perfusate cells at the PA and LA ports over time, which equalized at 60 minutes after injection. (c) The percentage of Tregs remaining in the circuit at the end of EVLP was calculated as $100 \times (\text{live cell count in the perfusate}) \times (\text{fraction of Tregs in live perfusate cells}) / (\text{number of injected cells})$, $p = 0.5886$, $R^2 = 0.03028$, $Y = -1.477 \times X + 26.67$. Linear regression. (d) Compliance, (e) Vascular resistance (VRES), (f) Mean pulmonary arterial pressure (PAP) of the donor lungs on EVLP, and (g) ratio of the partial pressure of oxygen in the perfusate (PaO₂) to the fraction of inspired oxygen (FiO₂) of allogeneic F344 lungs during EVLP with or without Treg injection. WKy, Wistar Kyoto; Treg, regulatory T cell; F344, Fisher 344; EVLP, ex vivo lung perfusion; PA, pulmonary artery; LA, left atrium; VRES, vascular resistance; PAP, pulmonary artery pressure.

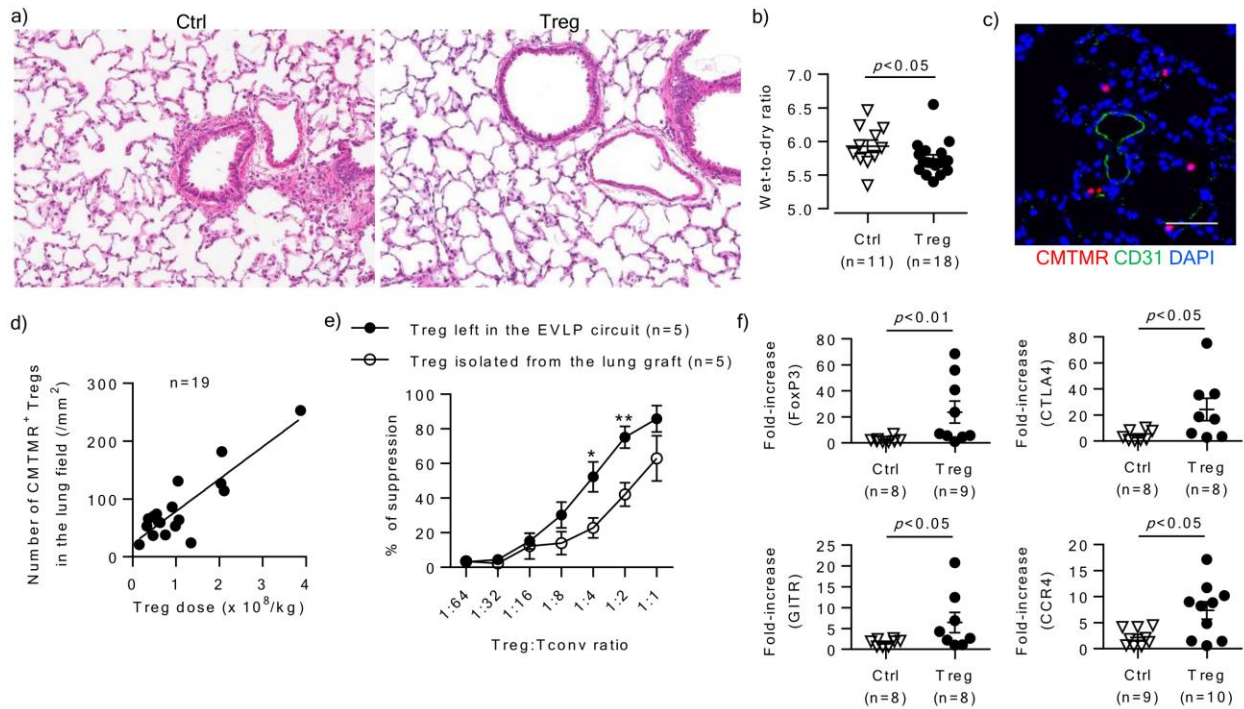


Figure 4. Expanded WKy Tregs enter allogeneic F344 lungs during EVLP while maintaining their regulatory function and phenotypic properties.

(a) Representative histology of the lung graft after EVLP (hematoxylin and eosin staining; $\times 40$).

(b) Wet-to-dry weight ratio in Treg-treated and control lungs. Control grafts were significantly heavier than Treg-treated ones ($p < 0.05$, Mann-Whitney U test). (c) Immunofluorescence staining of the lung graft after EVLP demonstrates CMTMR⁺ (red) Tregs located in the lung

tissue outside CD31⁺ (green) vessels. Scale bar = 25 μ m. (d) The number of CMTMR⁺ cells in the lung parenchyma was correlated with the injected dose of Tregs ($p < 0.0001$, $R^2 = 0.7542$, $Y = 0.5580 \times X + 22.75$). Linear regression.

(e) Tregs sorted from perfusate ($n = 5$) and digested lung tissue ($n = 5$) at the end of EVLP exhibited dose-dependent suppressive activity toward autologous Tconv ($p = 0.0001$ and $p < 0.0001$ for Tregs isolated from the lung graft and those left in the EVLP circuit, respectively; one-way ANOVA). At 1:4 and 1:2 of Treg:Tconv ratio,

Tregs left in the EVLP circuit showed better suppression than those isolated from the lung graft

(*: $p < 0.05$, **: $p < 0.01$, two-way repeated measures ANOVA) (f) Treg-related transcripts in the lung graft after EVLP, represented as a fold-increase based on house-keeping gene. FoxP3, CTLA4, GITR, and CCR4 expression were significantly increased in the lung graft of Treg-treated animals compared to control cases. Mann-Whitney U test was applied to compare the groups. WKy, Wistar Kyoto; Treg, regulatory T cell; F344, Fisher 344; EVLP, *ex vivo* lung perfusion; Tconv, conventional T cells.

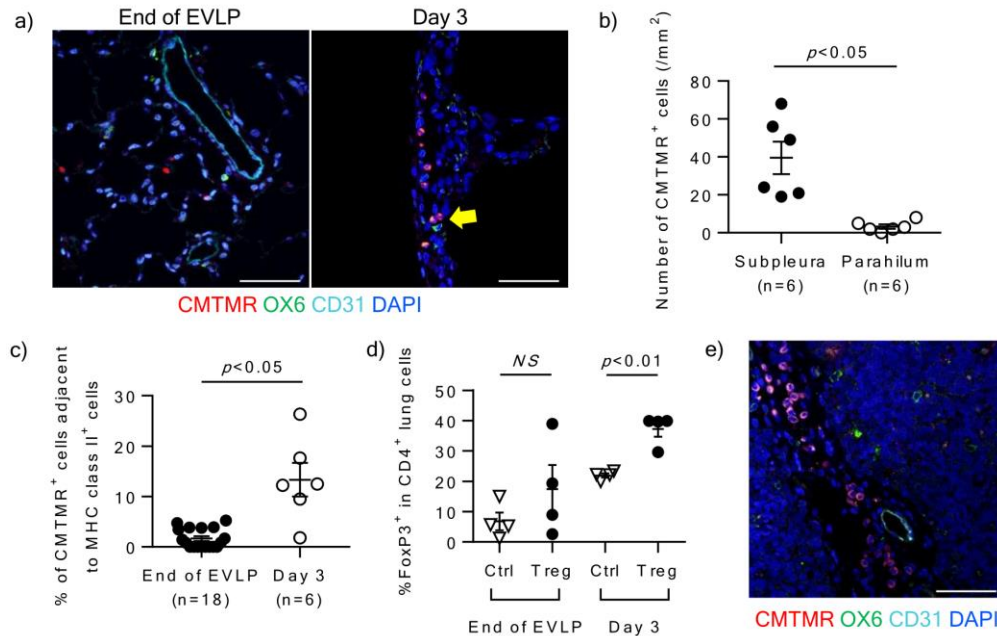


Figure 5. Tracking Tregs in the recipient after lung transplantation.

(a) Compared to at the end of EVLP, on day 3 post-transplant transferred CMTMR⁺ Tregs (red) were predominantly located in the subpleural area (< 50 μm from pleural surface) and often seen in proximity to MHC class II⁺ (green) cells (yellow arrow). Images from each channel are shown in supplementary figure 3a-b. Scale bars = 50 μm . (b) Spatial distribution of Tregs in the graft on day 3 ($p < 0.05$, Mann-Whitney U test), and (c) increased proximity of Tregs to MHC class II⁺ cells on day 3 ($p < 0.05$, Mann-Whitney U test). (d) The proportion of intragraft CD4⁺ T cells expressing Foxp3 was increased in Treg-treated grafts compared to controls at day 3 post-transplant ($p < 0.01$, Welch's T test). Gating strategy to identify intragraft CD4⁺ T cells and the representative histograms of FoxP3 expression in them are shown in supplementary figure 3c and supplementary figure 3d, respectively. N = 4 per group. (e) Identification of CMTMR⁺ Tregs (red) in the mediastinal lymph nodes of recipients of Treg-treated lung allografts on day 3. Images from each channel are shown in supplementary figure 3e. Scale bar = 50 μm . Treg, regulatory T cell; EVLP, ex vivo lung perfusion; MHC, major histocompatibility complex.

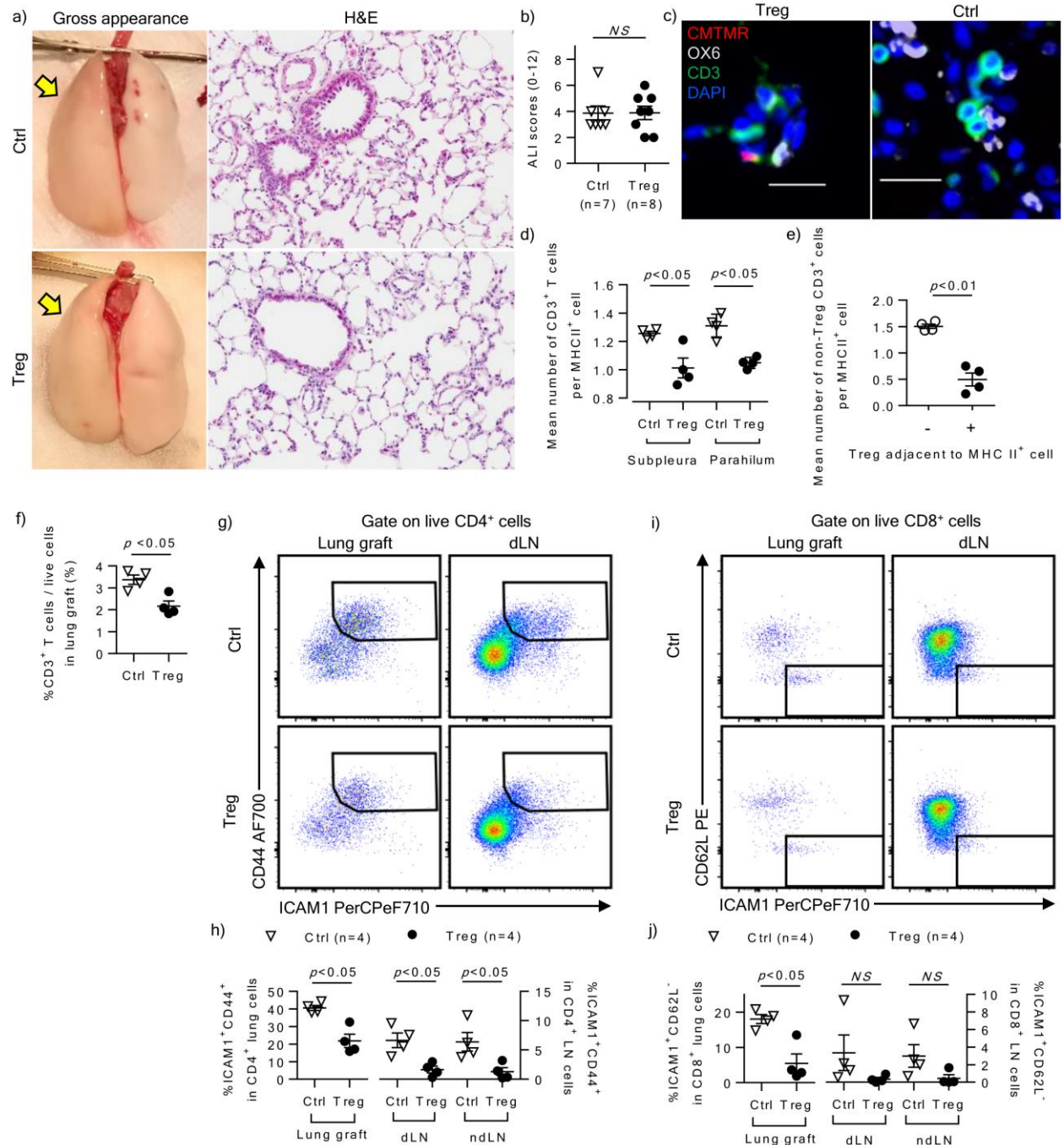


Figure 6. Post-transplant immune regulation by expanded Tregs delivered to the allograft prior to transplantation.

(a) Representative pictures of the gross appearance and the histology (hematoxylin and eosin staining; $\times 40$) of the lung graft (yellow arrows) on day 3 post-transplant. (b) ALI scores in Treg-

treated and control grafts. Details of histological semi-quantification are shown in supplementary figure 4a. (c) Representative high power immunofluorescence images showing intra-graft MHC class II⁺ cells (white) adjacent to CMTMR⁻CD3⁺ non-transferred Tconv (green) and CMTMR⁺CD3⁺ transferred Tregs (red). Scale bars = 20 μ m. (d) Mean number of CD3⁺ T cells adjacent to MHC class II⁺ cells in at least 10 high powered fields in Treg-treated and control lungs at the subpleural and perihilar areas. N = 4 per group. (e) Number of Tconv adjacent to MHC class II⁺ cells without (-) or with (+) an adjacent Treg cell (paired t test applied). N = 4 per group. (f) Percentage of CD3⁺ T cells (gating strategy shown in supplementary figure 4b), as well as CD4⁺ T cells and CD8⁺ T cells (supplementary figure 4c), was significantly decreased in Treg-treated lung graft on day 3. (g) Flow cytometric analysis of CD44 and ICAM1 expression on CD4⁺ cells from the lung allograft and dLN. (h) Percentage of ICAM1⁺CD44⁺ cells in the CD4⁺ T cell compartment in the lung, dLN and ndLN at day 3. (i) Flow cytometric analysis of CD62L and ICAM1 expression on CD8⁺ cells from the lung allograft and dLN. (j) Percentage of ICAM1⁺CD62L⁻ cells in the CD8⁺ T cell compartment in the lung, dLN and ndLN at day 3. Treg, regulatory T cell; ALI, acute lung injury; MHC, major histocompatibility complex; Tconv, conventional T cells; dLN, draining lymph node; ndLN, non-draining lymph node. Mann-Whitney U test was applied to compare the groups unless otherwise specified.

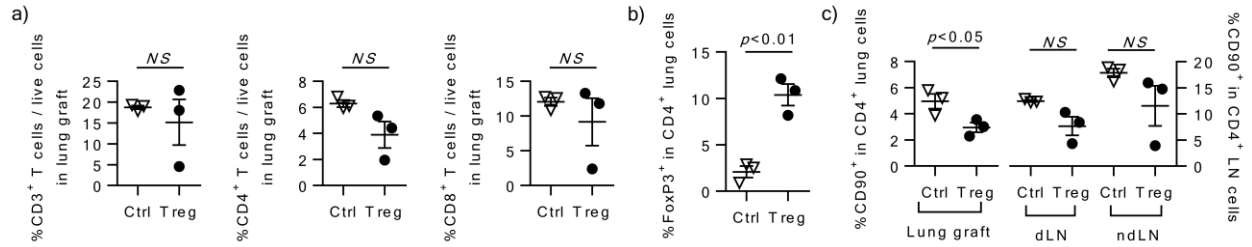


Figure 7. Suboptimal control of Tconv response in the lung at 7 days post-transplant.

(a) Percentage of T cells in Treg-treated lung graft on day 7. Gating strategy is shown in supplementary figure 5c. N = 3 per group. (b) Percentage of FoxP3⁺ in CD4⁺ T cells was significantly increased in Treg-treated lung graft on day 7, compared to control lungs. N = 3 per group. (c) CD90 expression on CD4⁺ T cells was significantly decreased in the lung graft of Treg-treated animals compared to control cases, but not statistically significant in dLN and ndLN. N = 3 per group. Analysis of FoxP3 and CD90 expression in CD4⁺ T cells is shown in supplementary figure 5d. Treg, regulatory T cells; dLN, draining lymph node; ndLN, non-draining lymph node. Mann-Whitney U test was applied to compare the groups.

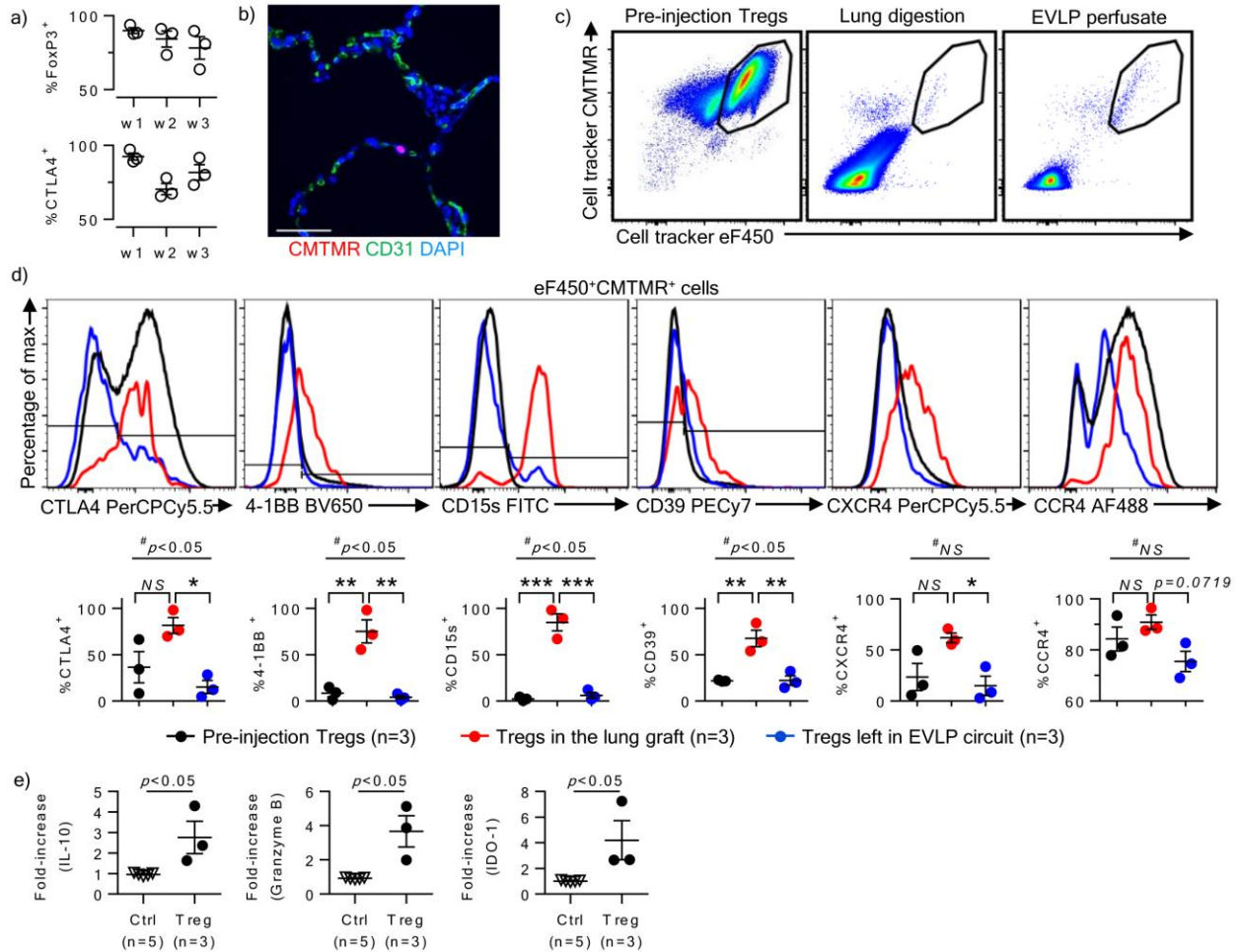


Figure 8. Delivery of human Tregs to allogeneic human lungs during EVLP.

(a) Expression of FoxP3 and CTLA4 during 21 days of expansion. N = 3 per group. (b) Immunofluorescence staining of the lung graft 1 hour after Treg administration. CMTMR⁺ cells (red) were identifiable in the parenchyma. Images from each channel are shown in supplementary figure 6c. Scale bar = 50 μ m. (c) Flow cytometric analysis of Tregs before injection (left panel), in the lung graft (middle panel) and in the perfusate (right panel) 1 hour after injection. (d) Analysis of the expression of the indicated markers on eF450⁺CMTMR⁺ cells in prior to injection (black lines), in the perfusate (blue lines) and in the lung allograft (red lines) 1 hour after injection, and those left in the EVLP circuit. N = 3 per group. Repeated measures (RM) one-way ANOVA revealed that there were significant differences in the expression of

CTLA4, 4-1BB, CD15s, and CD39 on Tregs between the groups. The expression of CXCR4 ($p = 0.0339$) and CCR4 ($p = 0.0719$) was higher on Tregs in the lung graft than in those left in EVLP circuit (Tukey's test), although the intergroup difference was not significant. The majority of Tregs in the lung graft was positive for CCR4 ($90.9 \pm 2.8\%$). #: RM ANOVA. *: $p < 0.05$, **: $p < 0.01$, ***: $p < 0.001$, Tukey's test. (e) Quantitative PCR analysis of the indicated transcripts in lung tissue. Transcripts measured at the end of EVLP and normalized to the housekeeping gene PPIA are displayed as a ratio to their abundance at the beginning of EVLP. Results from Treg-treated lungs ($n = 3$, red) are compared to results from untreated contemporaneous discarded lungs at the beginning and end of EVLP ($n = 5$, blue lines). Mann-Whitney U tests, $p < 0.05$ for IL-10, granzyme B and IDO-1. Treg, regulatory T cell; EVLP, *ex vivo* lung perfusion; PBMC, peripheral blood mononuclear cells; RM ANOVA, repeated measures ANOVA.

Supplementary Appendix Material

Supplementary Materials and Methods

Supplementary figure 1

Supplementary figure 2

Supplementary figure 3

Supplementary figure 4

Supplementary figure 4 extended

Supplementary figure 5

Supplementary figure 6

Supplementary table 1

Supplementary table 2

Supplementary table 3

Supplementary table 4

Supplementary movie 1

List of Abbreviations

ANOVA: Analysis of variance

ALI: Acute lung injury

APC: Antigen-presenting cell

CCR: C-C chemokine receptor

CD: Cluster of differentiation

CFSE: Carboxyfluorescein succinimidyl ester

CIT: Cold ischemic time

CXCR: C-X-C chemokine receptor

CLAD: Chronic lung allograft dysfunction

CMTMR: (5-(and 6-)-(((4-chloromethyl)benzoyl)amino)tetramethylrhodamine)

Ct: Threshold cycle

CTLA4: Cytotoxic T lymphocyte antigen 4

dLN: Draining lymph nodes

eF450: eFluor 450

EVLP: *Ex vivo* lung perfusion

F344: Fischer 344

FACS: Fluorescence activated cell sorting

FBS: fetal bovine serum

FiO₂: Fraction of inspired oxygen

FoxP3: Forkhead box p3

GITR: Glucocorticoid-induced tumour necrosis factor receptor

ICAM-1: Intercellular adhesion molecule 1

IDO-1: Indoleamine 2,3-dioxygenase 1

IL: Interleukin

ISHLT: International Society for Heart and Lung Transplantation

LA: Left atrium

LN: Lymph node

Lt: Left

LTx: Lung transplantation

MHC: Major histocompatibility complex

ndLN: Non-draining lymph node

PA: Pulmonary artery

PaO₂: Ratio of the partial pressure of oxygen in the perfusate

PAP: Pulmonary artery pressure

PBMC: Peripheral blood mononuclear cell

PEEP: Positive end-expiratory pressure

PPIA: Petidylprolyl isomerase A

PV: Pulmonary vein

rhIL-2: Recombinant human IL-2

RM: Repeated measures

Rt: Right

RT1: Rat major histocompatibility complex

Tconv: Conventional T cell

TCR: T cell receptor

TGF-beta:

TIGIT:

Treg: Regulatory T cell

TUNEL: Terminal deoxynucleotidyl transferase dextyridine triphosphate nick end labeling

VRES: Vascular resistance

WIT: Warm ischemic time

WKy: Wistar Kyoto

ZO-1: Zonula occludens-1

***Ex vivo* delivery of regulatory T cells for control of alloimmune priming in the donor lung**

Authors: Ei Miyamoto, Akihiro Takahagi, Akihiro Ohsumi, Tereza Martinu, David Hwang, Kristen M. Boonstra, Betty Joe, Juan Mauricio Umana, Ke F. Bei, Daniel Vosoughi, Mingyao Liu, Marcelo Cypel, Shaf Keshavjee, Stephen C. Juvet*

Supplementary Materials and Methods

Purification of rat Tregs and T conv cells

WKy rat cervical, axillary, inguinal, mesenteric, and mediastinal lymph nodes were crushed through 70 μm cell strainers to yield single cell suspensions. Cells were subjected to osmotic shock in 2 mL of NH_4Cl RBC lysis buffer for 4 min at room temperature. After washing, cells were incubated with anti-CD8 (Abcam) and anti-CD20 antibodies (Thermo Fisher Scientific) for 10 min at 4°C. The cells were washed and incubated with anti-mouse IgG microbeads (Miltenyi Biotec) for 10 min at 4°C. Magnetically labelled cells were removed using an LD column (Miltenyi Biotec). CD8- and CD20-depleted cells labelled with anti-CD4 FITC and anti-CD25 PE antibodies prior to FACS sorting on a BD Biosciences FACSAria II or FACSAria III. As depicted in supplementary figure 1a, $\text{CD4}^+\text{CD25}^{\text{high}}$ cells, which corresponded to 1.2~1.6% of total cells, were sorted as Tregs. $\text{CD4}^+\text{CD25}^{\text{low}}$ cells were also collected as Tconv for Treg suppression assays (see below). A total of $0.221\sim 0.478 \times 10^6$ of sorted $\text{CD4}^+\text{CD25}^{\text{high}}$ cells were cultured at 0.025×10^6 cells/mL in X-VIVO15 serum-free hematopoietic cell media (Lonza) with 5% fetal bovine serum (FBS, Gibco), 50 μM 2-mercaptoethanol (Thermo Fisher Scientific), 100 units/mL penicillin (Gibco), and 100 $\mu\text{g}/\text{mL}$ streptomycin (Gibco), in the presence of 2500 IU/mL rhIL-2 (Proleukin, Chiron Therapeutics) and anti-rat CD3 and anti-rat CD28 coated microbeads (Miltenyi Biotec) at 1:40 cell-to-bead ratio. Tregs were expanded in culture for 7 days and were replenished on day 3 with fresh cell culture media containing 2500 IU/mL rhIL-2, diluting the cells to no more than 0.4×10^6 cells/mL. The polyclonally expanded cells were harvested on day 7 and prepared for injection as described below.

Details of rat Treg injection during rat EVLP followed by LTx

F344 rats were intubated under anesthesia with 2% Isoflurane (Fresenius Kabi) and ventilated with 50% oxygen. At spine position, after flushing with 20 mL cold Perfadex (XVIVO Perfusion), the heart and lung bloc was extracted and connected to the EVLP circuit (Isolated Perfused Lung

Systems, Harvard Apparatus, supplementary figure 1d-e) which was filled with 150 mL perfusate solution (Steen®, XVIVO Perfusion, Denver, CO) containing 10000 units Heparin, 50 mg methylprednisolone sodium, and 50 mg cefazolin sodium. Perfusion and ventilation commenced at 37°C under the following conditions: inspiratory/expiratory pressure: 9/4 cmH₂O; I/E: 50%; respiratory rate: 40 per min; 21% oxygen. The perfusate was deoxygenated in a fiber membrane (Harvard Apparatus TYPE D150) filled with a gas mixture of 92% nitrogen and 8% CO₂. The left atrial line pressure was maintained at 2 cmH₂O against the hilum. At 60 min of EVLP, Tregs labelled with (5-(and 6-)-((4-chloromethyl)benzoyl)amino)tetramethylrhodamine (CMTMR; CellTracker Orange) dye and/or eF450 cell tracker dye in 1 mL Steen or 1mL Steen containing no cells were injected into the EVLP circuit upstream of the lungs via the injection port. Perfusate was sampled just before Treg injection and at 5, 15, 30, 60, 120 and 180 min after Treg injection both upstream (PA port) and downstream (LA port) of the lung allograft. At 180 min after Treg injection, the heart and lung block was disconnected from the EVLP circuit and placed in cold Perfadex. After ventilating for less than 1 min with 50% oxygen and 2 cmH₂O positive end-expiratory pressure (PEEP), the trachea was clamped. The left and right lungs were separated, keeping the left lung inflated, and the right lung was used for gene, histology, cytokine, flow cytometric analyses. The left lung was prepared for transplantation with cuff technique on cold Perfadex in 60 min after end of EVLP. Recipient WKy rats were anesthetized with 2% Isoflurane and ventilated with 21% oxygen and 2 cmH₂O PEEP. After anastomosing the bronchus, pulmonary vein, and pulmonary artery, the lung graft was re-perfused 15 min after placing the graft into the left chest cavity, and the chest was closed. After recovering from anesthesia, the recipients were administered 10 ug/kg buprenorphine subcutaneously. During euthanasia at day 3 or day 7 post-transplant, recipients were anesthetized with 2% Isoflurane.

In vitro rat Treg suppression assay

Polyclonally expanded Tregs and freshly sorted Tconv were labelled with cell proliferation dye eFluor 450 (eF450, Invitrogen) and Vybrant CFDA SE Cell Tracer Kit (CFSE, Invitrogen) according to the manufacturer's instructions, respectively. A total of 25×10^3 of Tconv were co-cultured in duplicate with varying numbers of Tregs in AIM-V medium (Thermo Fisher Scientific) with 50 μ M 2-mercaptoethanol, 100 units/mL penicillin, and 100 ug/mL streptomycin, in the presence of 1500 IU/mL rhIL-2 and anti-rat CD3/anti-rat CD28 coated microbeads at 1:2 of cell to bead ratio. After 96 hours, cells were stained for flow cytometric analysis on a BD Biosciences LSRII. The CD4⁺CFSE⁺ population in the eF450⁻FoxP3⁻ live cell gate was analyzed as Tconv as shown in supplementary figure 1c. Results were reported as percentage suppression, as described in figure 2b.

Isolation and expansion of human Tregs

Approximately 100 mL of whole blood was collected from a healthy donor under Institutional Research Ethics Board protocol 17-6229, and PBMCs were isolated using Lymphoprep (STEMCELL TECHNOLOGIES) according to the manufacturer's instructions. First, CD4⁺ cells were isolated by magnetic depletion of CD8⁺, CD14⁺, CD15⁺, CD16⁺, CD19⁺, CD36⁺, CD56⁺, CD123⁺, TCR γ δ ⁺, and CD235⁺ using a CD4⁺CD25⁺ T Cell Isolation Kit (Miltenyi Biotec). The isolated cells were labelled with anti-CD4, anti-CD25, and anti-CD127 antibodies and then CD4⁺CD25⁺CD127^{low} cells were isolated as human Tregs using FACS sorting on a BD FACSAria II or FACSAria III (supplementary figure 6a). Sorted Tregs were cultured in X-VIVO15 with 5% human AB serum in the presence of anti-human CD3/anti-human CD28 microbeads (Miltenyi Biotec) at a 1:2 cell-to-bead ratio and 500 IU/mL rhIL-2. The cells were expanded for 3 weeks during which they were replenished with 500 IU/mL rhIL-2 every 3~4 days diluting the cells to a density of $3-5 \times 10^5$ /mL. The cells were restimulated with anti-human CD3/anti-human CD28 microbeads (1:2 cell-to-bead ratio) at day 14. At day 21, when the cells had expanded ~1000-fold

(1~2 × 10⁹ cells), Tregs were resuspended in 50 mL of freezing media (90% FBS and 10% dimethylsulfoxide) and stored in liquid nitrogen for 16-100 days until needed.

Details of expanded human Treg injection during EVLP

The lung was perfused with Steen solution at 37°C , and ventilated with 21% oxygen, 5 cmH₂O PEEP, 8 mL/kg tidal volume (supplementary figure 6b), as previously described.¹ After 3 hours of lung assessment on EVLP, at which time the decision not to transplant the lung was made by the clinical team on the basis of organ quality,² cryopreserved Tregs were thawed, assessed for viability, and labelled with CMTMR and eF450 dyes according to the manufacturer's instructions.

Flow cytometry

Rat lymphocytes were obtained by crushing spleen and lymph nodes through 70 µm cell strainers. Human and rat lung cells were prepared by digesting the lungs in 4.5 mL HBSS with 2% FBS, 10 mg/mL Collagenase A (Sigma Aldrich), and 10 mg/mL DNase (Sigma Aldrich) with gentleMACS dissociator (Miltenyi Biotec) and subsequently filtering through 70 µm cell strainer. Clones and species for antibodies used for flow cytometry were described in Table S3. All samples were fixed using a transcription factor fixation and permeabilization buffer set (eBioscience) according to the manufacturer's instructions and run on an LSRII. Data were analyzed with FlowJo software (FlowJo, LLC).

Tissue section staining and histological assessment

Tissue samples were fixed in 10% neutral buffered formalin and embedded in paraffin. 5 µm sections were stained with hematoxylin-eosin, immunohistochemical, or immunofluorescence stains. Clones and species for antibodies used for immunohistochemistry and immunofluorescence stains were described in Table S4. ImmPRESS™ Anti-rabbit IgG reagent (Vector Labs) and liquid DAB+ substrate chromogen solution (DAKO) were used for immunohistochemistry. Analysis of stained sections were performed by blinded observers (D.H.

for ALI score, K.F.B. and S.J. for ZO-1 score, and D.V. for Tconv-Treg-APC analysis). ALI score (0-12) was assessed as a sum of 4 categories: alveolar space hemorrhage (0-3), vascular congestion (0-3), edema/fibrin (0-3), and interstitial white cells (0-3). Infiltration of the inflammatory cells to the peri-vascular area (A grade) and peri-bronchiole area (B grade) of the lung graft was assessed based on the criteria proposed by International Society of Heart and Lung Transplantation.³ For zonula occludens-1 (ZO-1) score, ZO-1 alveolar cell membrane staining intensity in 5 randomly selected images from each lung was determined in a semiquantitative manner (0-4), as previously described.⁴ The results were evaluated by two independent blinded investigators (K.F.B. and S.J.) and averaged. For Tconv-Treg-APC analysis, scanned images from 10 randomly selected locations from each lung were obtained. The average number of Tconv cells (CMTMR⁻CD3⁺) adjacent to MHC class II⁺ cells associated with, and not associated with, transferred Tregs (CMTMR⁺CD3⁺) was determined.

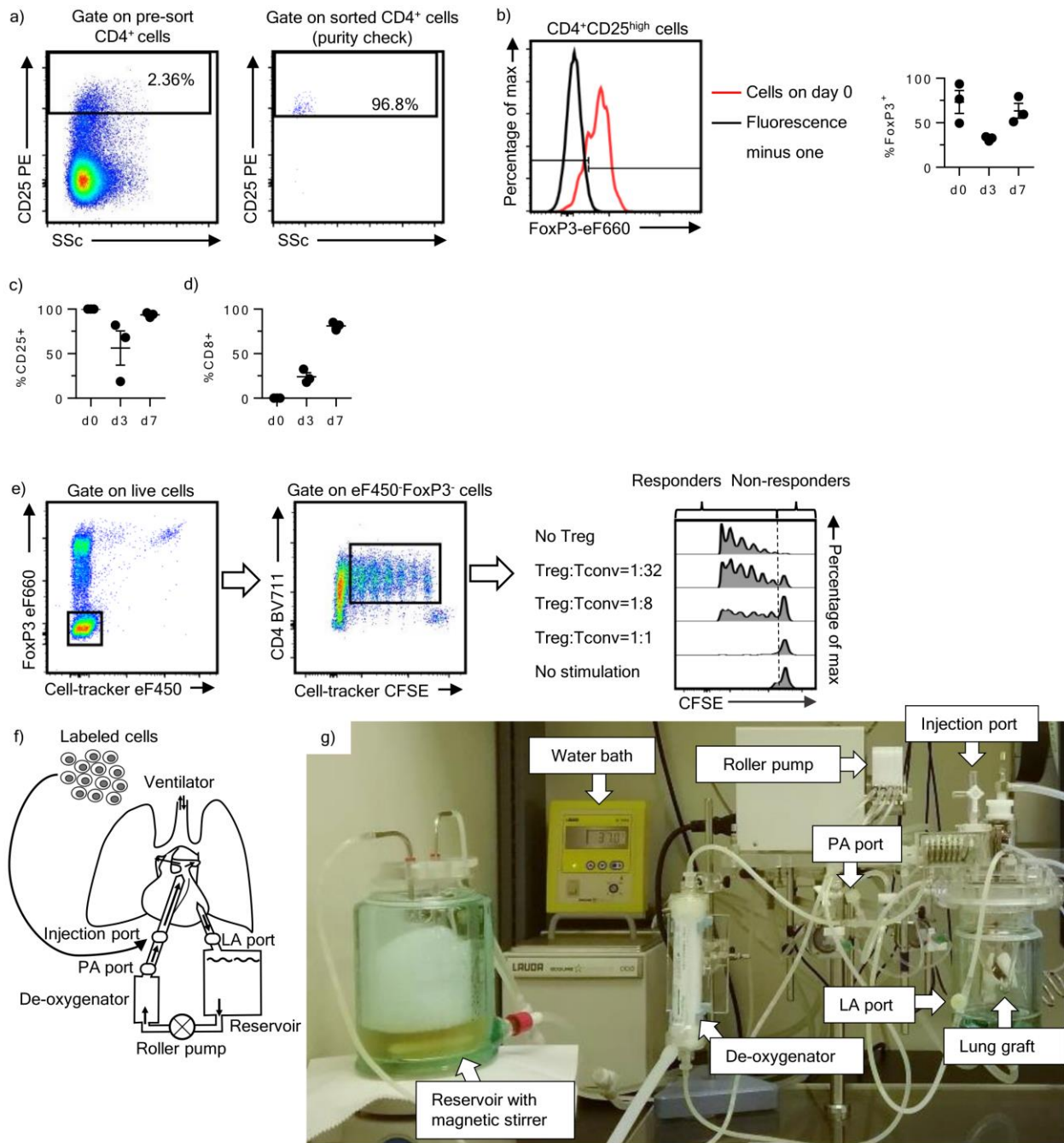
Gene transcript analysis

Lung and lymph node samples were put in RNAlater stabilization solution (Invitrogen) for 4~7 days and then stored in -80 °C. Total RNA was extracted from the tissue using RNeasy Mini Kit (Qiagen) and converted into cDNA using an iScript Select Kit (Bio-Rad Laboratories, Hercules CA). SsoAdvanced Universal SYBR Green Supermix (Bio-Rad) and a Bio-Rad CFX384 Tough real-time PCR thermal cycler were used for PCR. Primers were designed across introns. Threshold cycle (Ct) values were determined using instrument software. Changes in gene expression were calculated using the $2^{-\Delta\Delta Ct}$ method with normalization to expression of peptidylprolyl isomerase A.

Supplementary References:

1. Cypel M, Yeung JC, Hirayama S, et al. Technique for Prolonged Normothermic Ex Vivo Lung Perfusion. *J Hear Lung Transplant* 2008;27:1319-1325.
2. Cypel M, Yeung JC, Mingyao L, et al. Normothermic ex vivo lung perfusion in clinical lung transplantation. *N Engl J Med* 2011;364:1431-1440.
3. Stewart S, Fishbein MC, Snell GI, et al. Revision of the 1996 Working Formulation for the Standardization of Nomenclature in the Diagnosis of Lung Rejection. *J Hear Lung Transplant* 2007;26:1229-1242.
4. Cypel M, Liu M, Rubacha M, et al. Functional repair of human donor lungs by IL-10 gene therapy. *Sci Transl Med* 2009;1:4ra9.

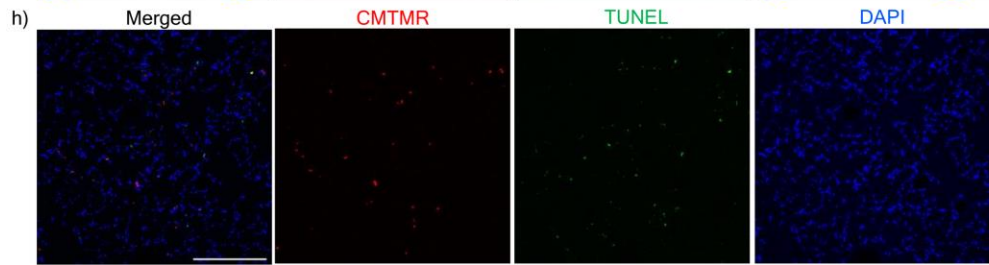
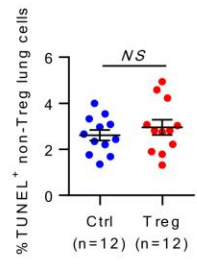
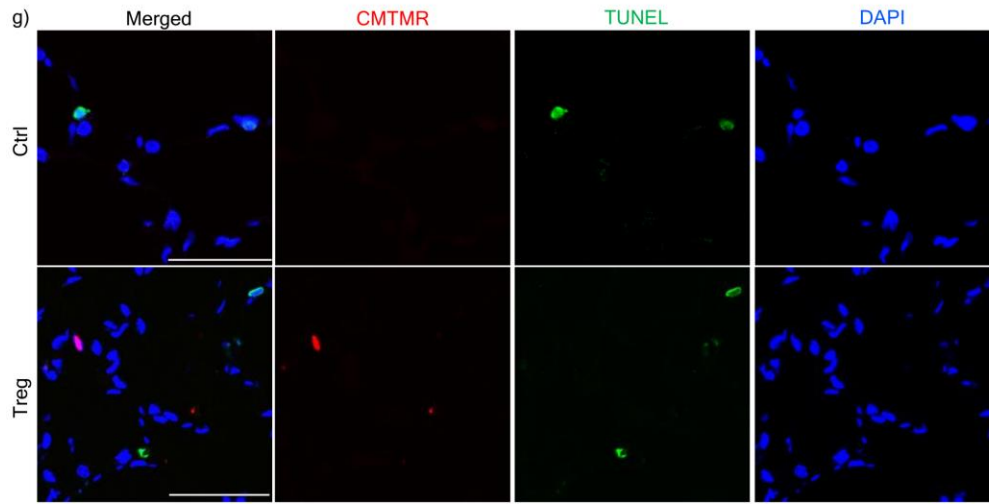
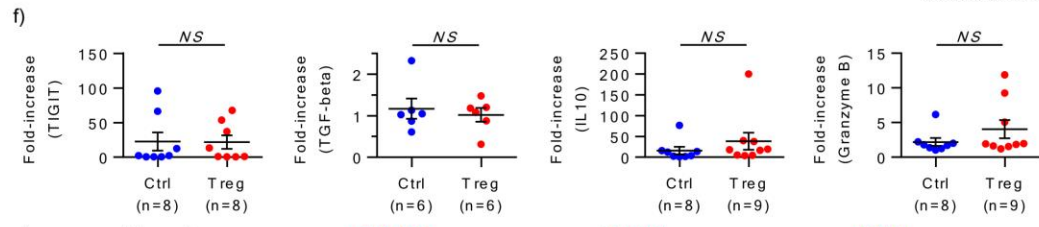
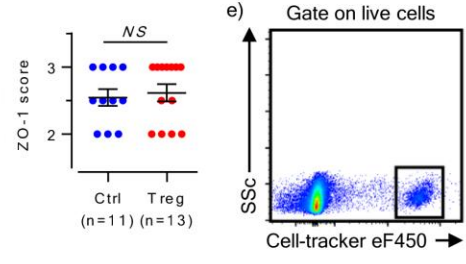
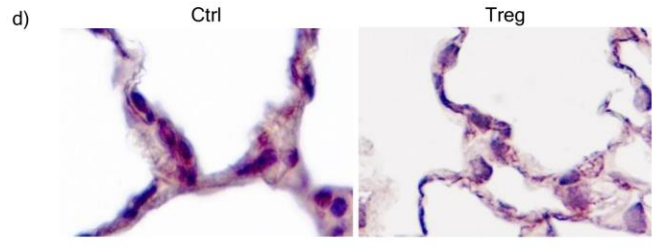
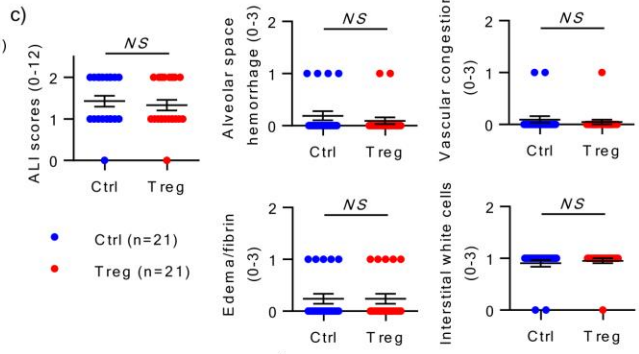
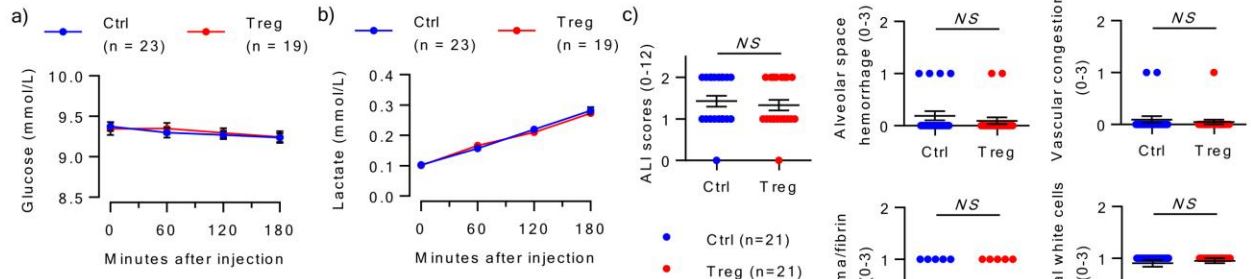
Supplementary figure legends



Supplementary figure 1. Rat Treg and EVLP procedures

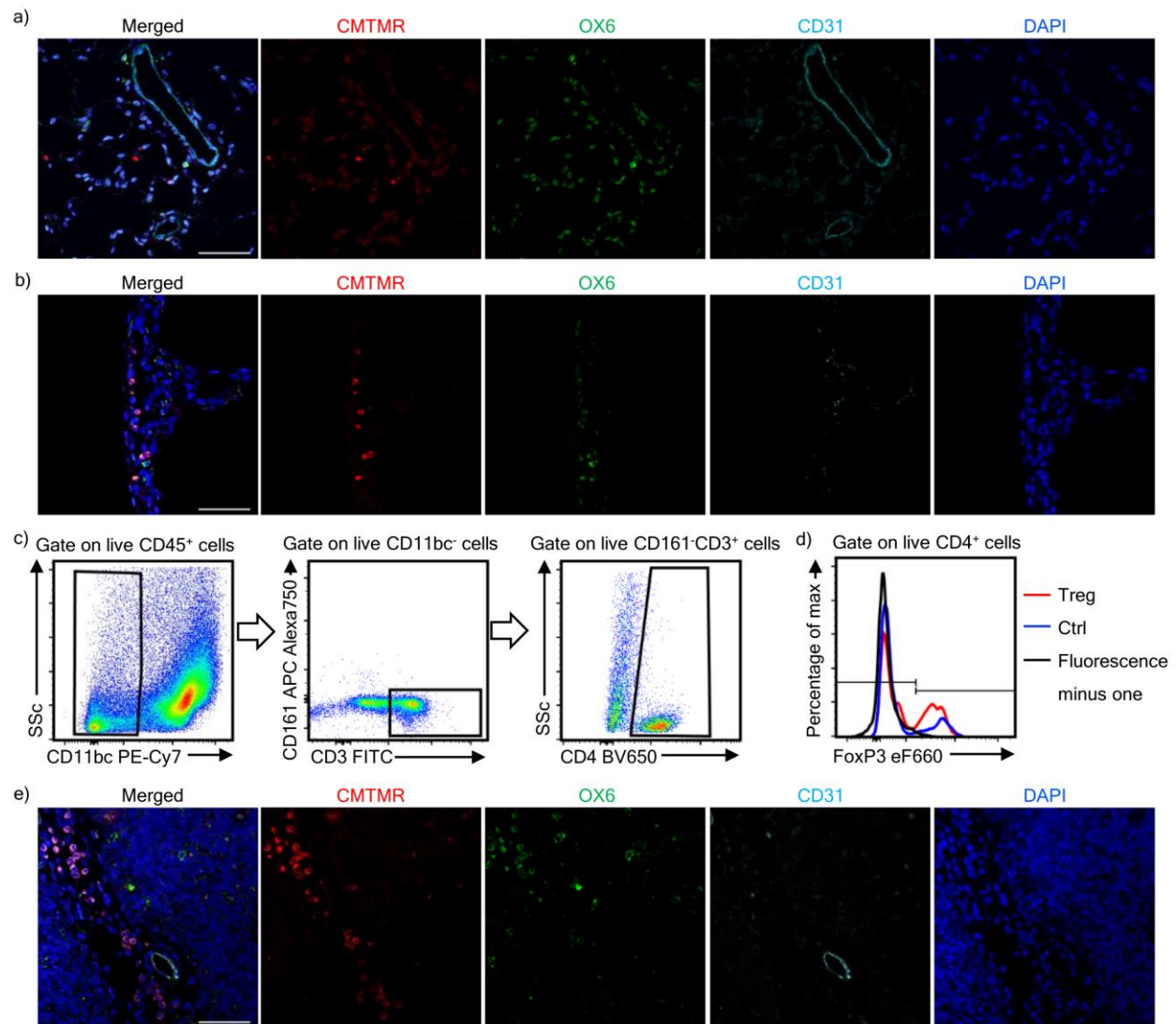
(a) WKy rat Treg isolation. After magnetic depletion of CD8⁺ and CD20⁺ cells, the top 2% of CD25⁺ cells in the CD4⁺ gate were sorted by FACS. $91.6 \pm 1.4\%$ of the sorted cells were positive for both CD4 and CD25 (n = 5). (b) 76.8% of the sorted cells were positive for FoxP3

(left panel). FoxP3 expression decreased on day 3 and then returned to the similar level of day 0 by day 7 (right panel, n = 3). (c) CD25 expression in the rat Tregs during the culture (n = 3). (d) CD8 expression increased in the rat Tregs over the 7 days of culturing (n = 3). (e) Representative gating to identify conventional T cells (Tconv cells) at condition of Treg:Tconv = 1:32. eF450⁺FoxP3⁻CFSE⁺CD4⁺ population was considered as Tconv cells. In the right panel, histograms of CFSE intensity in WKy FoxP3⁻ CD4⁺ T cells (Tconv cells) following 4 days of culture with or without autologous expanded Tregs. Percent suppression was calculated as $100 \times \{(\%Tconv \text{ with Treg} - \%Tconv \text{ without Treg})/\%Tconv \text{ without stimulation}\}$. (f) Expanded Tregs were injected in 1 mL of Steen solution at the injection port located upstream of the donor lungs. In control cases, 1 mL of Steen solution (no cells) was injected. Perfusate samples were collected from the PA and LA ports. After disconnecting the donor lungs from the circuit at the end of EVLP, the remaining perfusate in the circuit was collected. (g) Picture of rat EVLP system. See supplementary movie 1. Treg, regulatory T cell; EVLP, *ex vivo* lung perfusion; PA, pulmonary artery; LA, left atrium.



Supplementary figure 2. The effect of Treg injection during EVLP on the lung graft.

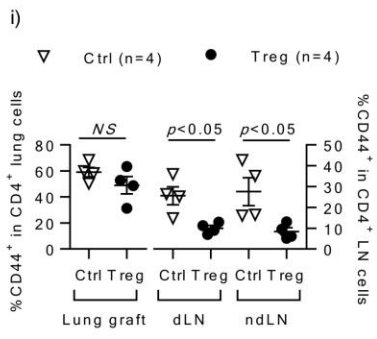
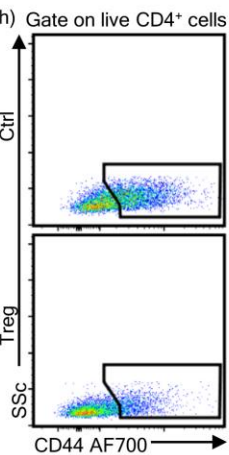
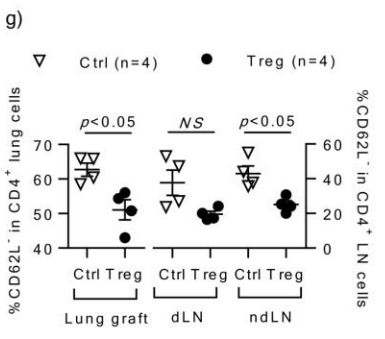
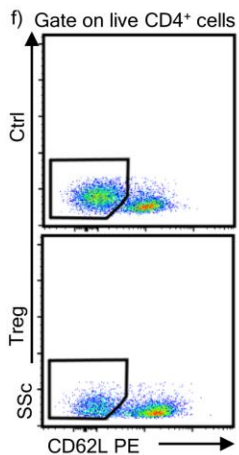
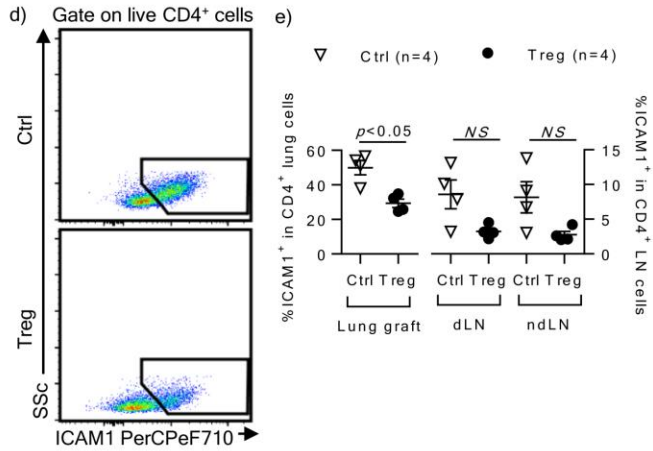
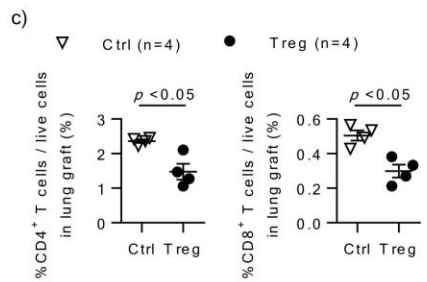
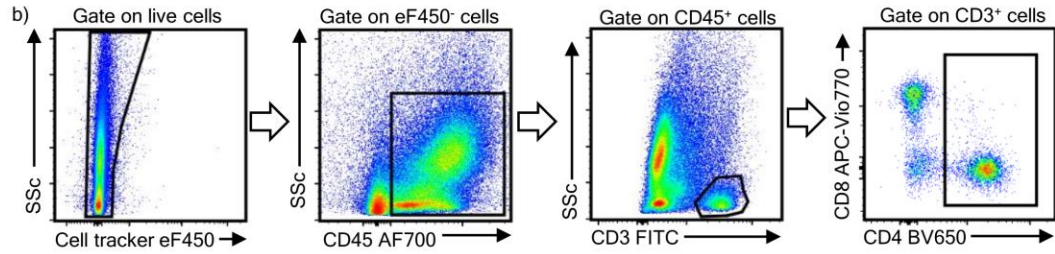
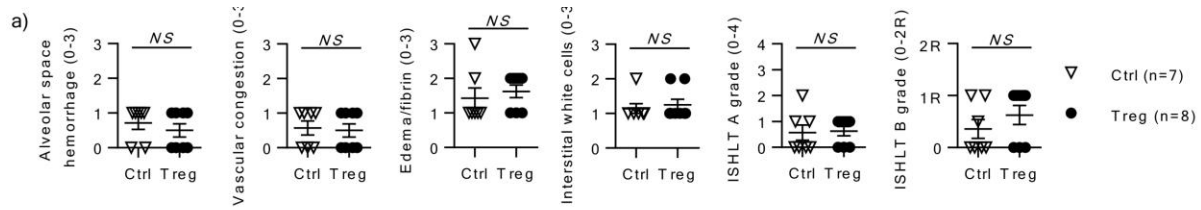
(a) Glucose level in the LA perfusate during EVLP. (b) Lactate level in the LA perfusate during EVLP. (c) ALI score (0-12) was an aggregate score which was derived by semi-quantification of alveolar space hemorrhage, vascular congestion, interstitial edema/fibrin deposition, and interstitial infiltration of white blood cells. (d) Representative pictures of ZO-1 staining ($\times 100$, $p = \text{NS}$). (e) Identification of transferred Tregs in the digested lung by flow cytometry. (f) Treg-related transcripts in the lung graft after EVLP, represented as a fold-increase and normalized to the house-keeping gene peptidylprolyl isomerase A (PPIA). There were no significant differences in TIGIT, TGF-beta, IL-10, or Granzyme B expression between the lung grafts of Treg-treated animals and control cases. (g) TUNEL-positive apoptotic lung cells (green) in the lung after EVLP ($p = \text{NS}$, scale bars = 25 μm). (h) The percentage of TUNEL⁺ in CMTMR⁺ cells in the lung graft after EVLP was $0.97 \pm 0.52\%$ ($n = 11$, scale bar = 100 μm). CMTMR⁺ Tregs were not in the proximity of apoptotic cells. Treg, regulatory T cells; EVLP, *ex vivo* lung perfusion. LA, left atrium; ALI, acute lung injury. Mann-Whitney U test was applied to compare the groups.



Supplementary figure 3. Kinetics of the injected cells in the recipient after lung transplantation.

(a) Images show (left to right): merged image; CMTMR⁺ cells (red); OX6⁺ cells (rat MHC class II⁺ cells, green); CD31⁺ vessels (light blue); and nuclei (blue). (b) Images show (left to right): merged image; CMTMR⁺ cells (red); OX6⁺ cells (rat MHC class II⁺ cells, green); CD31⁺ vessels (light blue); and nuclei (blue). (c) Live CD45⁺CD11bc⁻CD161⁻CD3⁺CD4⁺ cells were considered as CD4⁺ T cells in flow cytometric analyses. (d) Analysis of FoxP3 expression in CD4⁺ in the lung graft on day 3. (e) Each channel visualized CMTMR⁺ cells (red), OX6⁺ cells (rat MHC class

II⁺ cells; green), CD31⁺ vessels (light blue), or nuclei (blue). Treg, regulatory T cells; EVLP, *ex vivo* lung perfusion; MHC, major histocompatibility complex. Scale bars = 50 μ m.

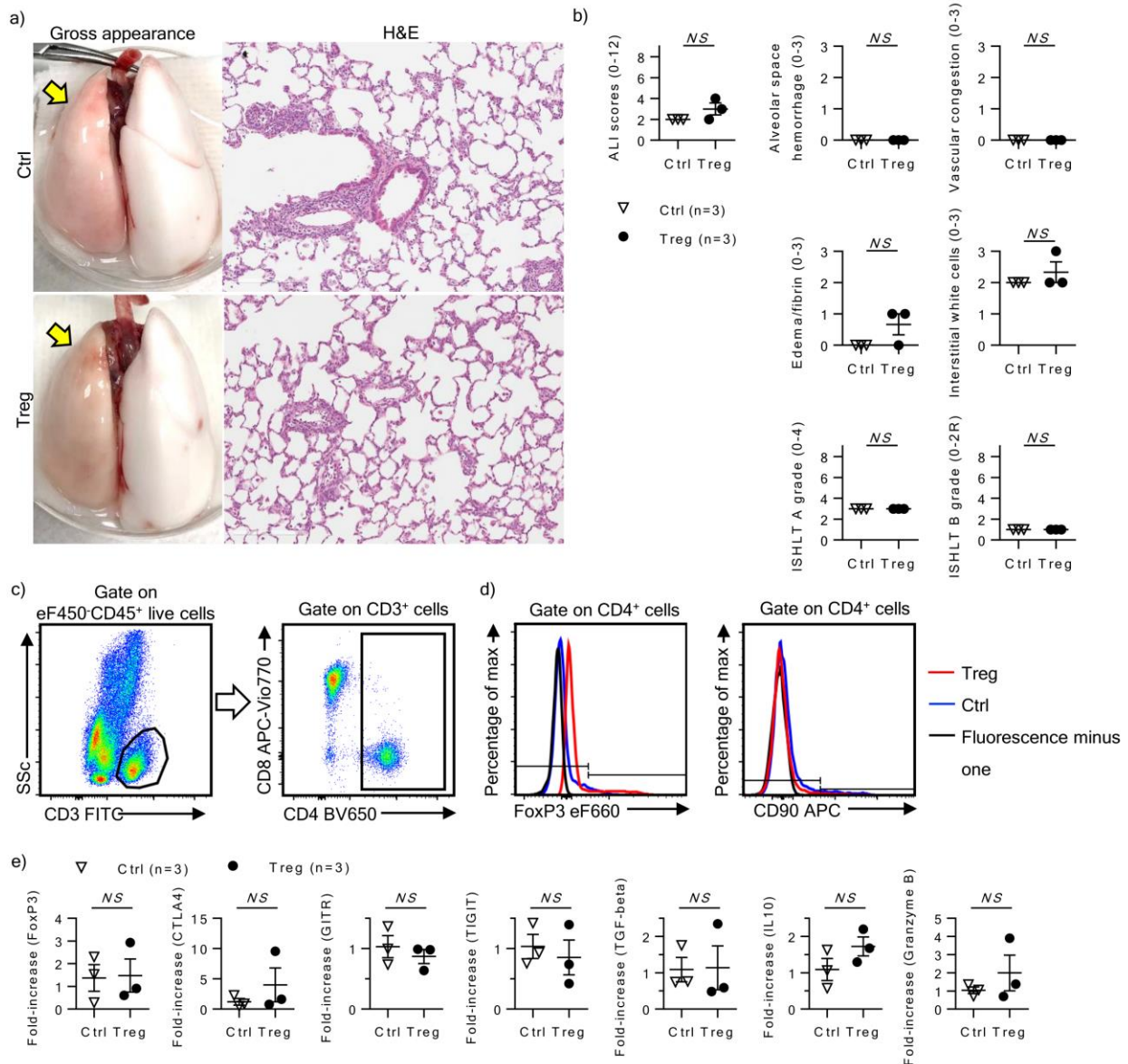


Supplementary figure 4. The immunomodulatory effect of Treg injection on the lung graft at day 3 post-transplant.

(a) Semi-quantification of alveolar hemorrhage, vascular congestion, interstitial edema/fibrin deposition, interstitial infiltration of white blood cells, ISHLT A grade (peri-vascular infiltration of inflammatory cells), ISHLT B grade (peri-bronchiole infiltration of inflammatory cells), and the percentage of inflammation area on day 3 post-transplant in Treg-treated and untreated lungs. (b) eF450⁻CD45⁺CD3⁺ cells were defined as non-transferred T cells. (c) The percentage of CD4⁺ (left panel) and CD8⁺ (right panel) cells in intra-graft live cells on day 3 was lower in Treg-treated animals than in controls ($p < 0.05$ and $p < 0.05$, respectively). (d) Representative FACS dot plot to identify the ICAM1⁺ population in CD4⁺ T cells. (e) ICAM1 expression on CD4⁺ T cells was significantly decreased in lung grafts of Treg-treated animals compared to control cases, but not in lymph nodes. (f) Representative FACS dot plot to identify the CD62L⁻ population in CD4⁺ T cells. (g) The CD62L⁻ population in CD4⁺ T cells was decreased in the lung graft of Treg-treated animals compared to control cases, but not in their draining lymph nodes. (h) Representative FACS dot plot to identify CD44⁺ population in CD4⁺ T cells. (i) CD44 expression on CD4⁺ T cells was decreased in lymph nodes of Treg-treated animals compared to control cases, but not in the lung graft. EVLP, *ex vivo* lung perfusion; Treg, regulatory T cells; ISHLT, international society of heart and lung transplantation; dLN, draining lymph node; ndLN, non-draining lymph node. Mann-Whitney U test was applied to compare the groups.

Supplementary figure 4 extended.

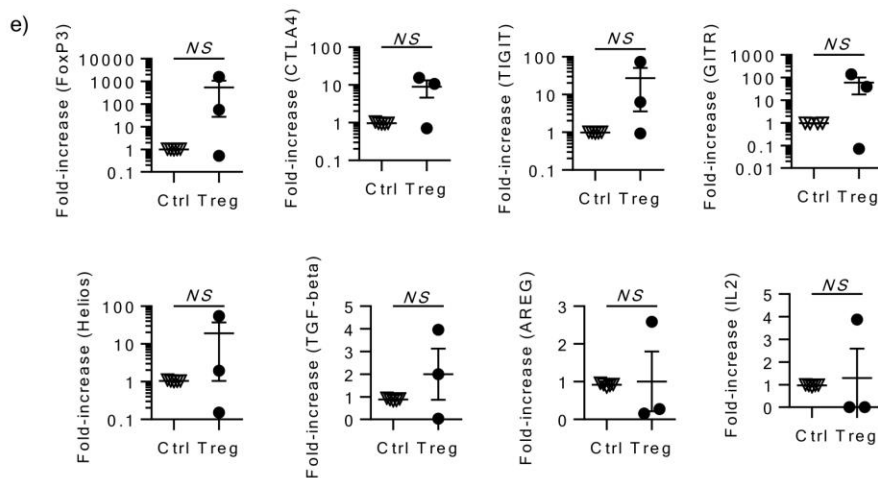
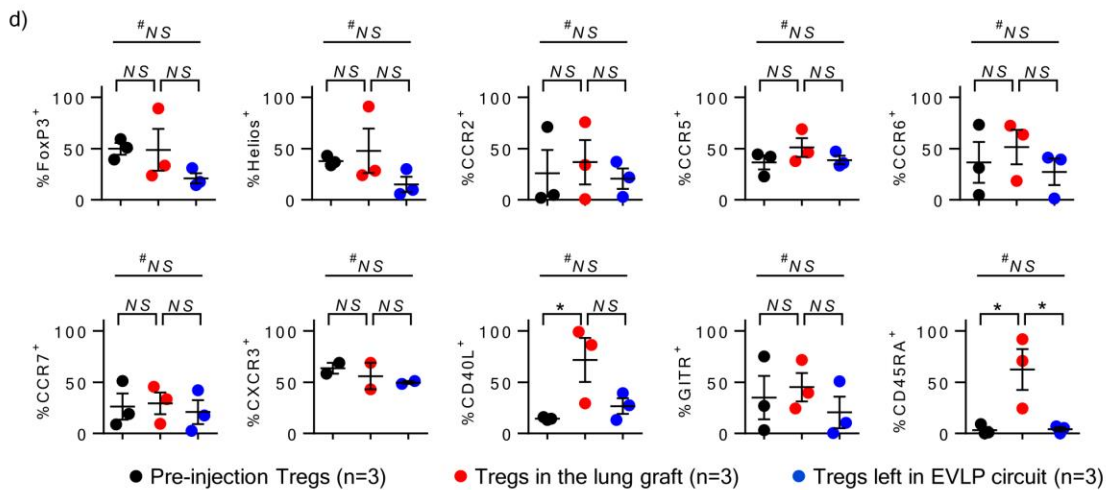
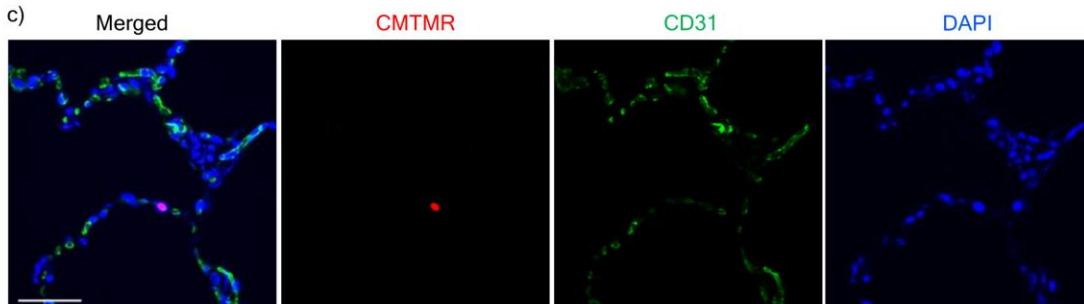
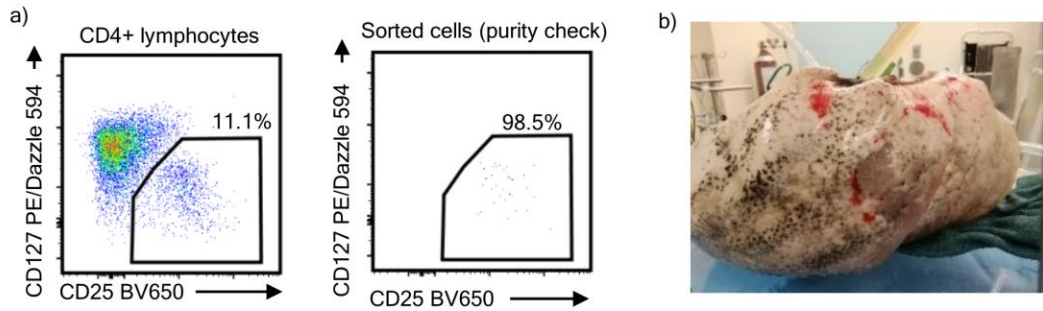
(j) Representative FACS dot plot to identify the ICAM1⁺CD62L⁻ population in CD4⁺ T cells. (k) The ICAM1⁺CD62L⁻ population of CD4⁺ T cells was decreased in the lung graft and lymph nodes of Treg-treated animals compared to control cases. (l) Representative FACS dot plot to identify the CD44⁺CD62L⁻ population in CD4⁺ T cells. (m) The CD44⁺CD62L⁻ population in CD4⁺ T cells was decreased in the lymph nodes of Treg-treated animals compared to control cases, but not in the lung graft. (n) Treg-related transcripts in the lung graft on day 3 post-transplant, represented as a fold-increase compared to the housekeeping gene PPIA. (o) FoxP3 expression in the lymph nodes of Treg-treated animals compared to control cases. Treg, regulatory T cells; EVLP, *ex vivo* lung perfusion; dLN, draining lymph node; ndLN, non-draining lymph node. Mann-Whitney U test was applied to compare the groups.



Supplementary figure 5. Administration of expanded Tregs during EVLP does not ameliorate lung allograft rejection at day 7 post-transplant.

(a) Representative pictures of the gross appearance and the histology (hematoxylin and eosin staining; $\times 40$) of the lung graft (yellow arrows) on day 7 post-transplant. (b) There were no intergroup difference in semi-quantification of ALI score which is the sum of alveolar space hemorrhage, vascular congestion, interstitial edema/fibrin deposition, and interstitial infiltration of white blood cells scores, ISHLT A grade, and ISHLT B grade in the lung grafts on day 7 post-

transplant. (c) The representative FACS dot plot to identify CD4⁺ and CD8⁺ T cell populations in the lung graft. (d) Analysis of FoxP3 and CD90 expression in CD4⁺ T cells in the lung graft on day 7 post-transplant. (e) Treg-related transcripts in the lung graft on day 7 post-transplant, represented as a fold-increase based on house-keeping gene. Treg, regulatory T cells; EVLP, ex vivo lung perfusion; ALI, acute lung injury; ISHLT, International Society of Heart and Lung Transplantation; FACS, fluorescence activated cell sorting. Mann-Whitney U test was applied to compare the groups.



Supplementary figure 6. Delivery of human Tregs to allogeneic human lungs during EVLP.

(a) CD4⁺CD25^{high}CD127^{low} cells were sorted from CD4-enriched PBMC as human Tregs.

Representative purity of the sorted cells is shown; overall 94.1 ± 2.2% of the sorted cells were found in CD25⁺CD127⁻ gate (n = 3). (b) Gross appearance of the donor right lung on EVLP. (c)

Each channel visualized CMTMR⁺ cells (red), CD31⁺ vessels (green), or nuclei (blue). There was strong signal from DAPI channel since the administered Tregs were labelled with eF450 cell-tracker dye for flow cytometric analysis as well as CMTMR for IF staining. CMTMR⁺ Tregs were resident in the outside of CD31⁺ capillaries. Tregs, regulatory T cells. Scale bar = 50 µm.

(d) Expression of FoxP3, Helios, CD40L, GITR, CD45RA, and chemokine receptors on Tregs taken from the lung and those remaining in the EVLP circuit 1h after Treg injection. #: analyzed by RM ANOVA. *: $p < 0.05$, analyzed by Tukey's test. (e) Quantitative PCR analysis of the

indicated transcripts in lung tissue. Transcripts measured at the end of EVLP and normalized to the housekeeping gene PPIA are displayed as a ratio to their abundance at the beginning of EVLP. Results from Treg-treated lungs (n = 3, red) are compared to results from untreated contemporaneous discarded lungs at the beginning and end of EVLP (n = 5, blue lines). Mann-

Whitney U test was applied to compare the groups. Tregs, regulatory T cells; FACS, fluorescence activated cell sorting; EVLP, *ex vivo* lung perfusion; PBMC, peripheral blood mononuclear cells; RM ANOVA, repeated measures ANOVA.

Supplementary table 1. The conditions of human Tregs and human lung EVLP

Variables	EX1	EX2	EX3
Number of sorted Tregs on day 0	1.40×10^6	1.30×10^6	1.87×10^6
Viability on day 21 before cryopreservation (%)	98.0	94.0	97.0
Duration of cryopreservation (days)	80	121	38
Number of Tregs injected (n)	0.5×10^9	0.8×10^9	0.4×10^9
Fold-expansion in 21 days	1307.1	1538.5	352.9
Number of Tregs injected (n)	0.5×10^9	0.8×10^9	0.4×10^9
Viability at injection (%)	87.2	89.0	85.8
PaO ₂ /FiO ₂ in EVLP perfusate just before Treg injection (mmHg)	406.4	373.0	433.7
PaO ₂ /FiO ₂ in perfusate 1h after Treg injection (mmHg)	406.1	346.8	339.3
Treg, regulatory T cell; PaO ₂ /FiO ₂ , ratio of the partial pressure of oxygen in the perfusate (PaO ₂) to the fraction of inspired oxygen (FiO ₂).			

Supplementary table 2. Clinical features of donor lungs in the human EVLP experiment.

Variables	Treg injection (n = 3)	Ctrl (n = 5)
Lung donor sex (female/male, n)	0/3	2/3
DCD/DBD (n)	2/1	3/2
EVLP type		
Rt. Single lung EVLP (n)	2	2
Lt. single lung EVLP (n)	1	0
Double lung EVLP (n)	0	3
Treg, regulatory T cell; Ctrl, control lungs for PCR analysis; DCD, donation after cardiac death; DBD, donation after brain death.		

Supplementary table 3. Antibodies for flow cytometry

Marker	Fluorochrome	Reactivity	Company	Clone	Dilution
CD3	FITC	Rat	BD Biosciences	G4.18	1/100
CD4	FITC	Rat	eBioscience	OX35	1/100
CD4	BV650	Rat	BD Biosciences	OX-35	1/100
CD4	BV711	Rat	BD Biosciences	OX-35	1/100
CD25	PE	Rat	eBioscience	OX39	1/100
CD25	BV650	Rat	BD Biosciences	OX-39	1/100
CD8a	PerCP-eF710	Rat	eBioscience	OX8	1/100
CD8a	APC-Vio770	Rat	Miltenyi Biotec	REA437	1/100
CD11b/c	PE-Cy7	Rat	BD Biosciences	OX-42	1/100
CD44	AF700	Rat	Novus biologicals	OX-50	1/100
CD45	AF700	Rat	Biolegend	OX-1	1/100
CD45	BV711	Rat	BD Biosciences	OX-1	1/100
CD62L	PE	Rat	BioLegend	OX-85	1/100
CD90	APC	Rat	BioLegend	OX-7	1/100
CD161	APC-Vio770	Rat	Miltenyi Biotec	REA227	1/100
CTLA4	Biotin	Rat	Thermo/invitrogen	WKH 203	1/100
ICAM1	PerCP-eF710	Rat	eBioscience	1A29	1/100

Rat Fc Block (anti-CD32)	-	Rat	BD Biosciences	D34-485	1/100
FoxP3	PE-eF610	Rat and human	eBioscience	FJK-16s	1/50
FoxP3	eF660	Rat and human	eBioscience	150D/E4	1/50
Viability	Fixable viability stain 700	Rat and human	BD Biosciences	-	1/1000
Viability	Fixable viability stain PE-CF594	Rat and human	BD Biosciences	-	1/1000
CD4	BV711	Human	BD Biosciences	SK3	1/100
CD8	APC/Cy7	Human	Biolegend	SK1	1/100
CD25	BV785	Human	Biolegend	BC96	1/100
CD127	PerCP-Cy5.5	Human	Biolegend	A019D5	1/100
GITR	APC/Fire750	Human	Biolegend	108-17	1/100
Helios	PE/Cy7	Human	Biolegend	22F6	1/50
CD40L	Biotin	Human	Biolegend	24-31	1/100
CD45RA	FITC	Human	Biolegend	HI100	1/100

CTLA4	PerCP-Cy5.5	Human	Biolegend	BNI3	1/100
4-1BB	BV650	Human	Biolegend	4B4-1	1/100
CD15s	FITC	Human	Biolegend	FH6	1/100
CD39	PE/Cy7	Human	Biolegend	A1	1/100
CCR2	BV605	Human	Biolegend	k036C2	1/100
CCR4	AF488	Human	R&D Systems	205410	1/100
CCR5	APC/Cy7	Human	Biolegend	J418F1	1/100
CCR6	Biotin	Human	BD Biosciences	11A9	1/100
CCR7	PE-Cy7	Human	BD Biosciences	3D12	1/100
CXCR3	BV 785	Human	Biolegend	G025H7	1/100
CXCR4	PerCP-Cy5.5	Human	Biolegend	12G5	1/100
Human Fc Block	-	Human	BD Biosciences	-	1/100

Supplementary table 4. Antibodies for IF and IHC

Marker	Host species	Reactivity	Company	Dilution	Application
OX-6	Mouse	Rat	BD bioscience	1/200	IF
CD31	Rabbit	Rat and human	abcam	1/300	IF
CD3	Rabbit	Rat	DAKO	1/200	IF
ZO-1	Rabbit	Rat	Invitrogen	1/300	IHC
IF, immunofluorescence staining; IHC, immunohistochemistry staining					

Supplementary movie 1. Rat heart-lung block perfused and ventilated during EVLP.